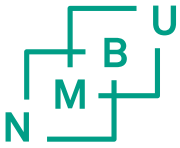
U
B
M
N

ACKNOWLEDGEMENTS

The present work was carried out at the Department of Chemistry, Biotechnology and Food Science at the Norwegian University of Life Science from January until May 2014 with professor Vincent Eijsink and associate professor Gustav Vaaje-Kolstad as supervisors.

First, I would like to thank my supervisors for excellent guidance during my work. Vincent, thank you for giving me the opportunity to write my thesis in the Protein Engineering and Proteomics (PEP) group and for your enthusiasm and ideas. Gustav, thank you for always being there to answer any of my questions, and for encouraging and inspiring me.

Thanks to all the members of the PEP group for creating a very pleasant work environment, and for helpful discussions. I am really looking forward to continue working in the group.

Finally, I would like to express my gratitude to my family and friends for their support and encouragement, and especially Jan Erik for your tremendous support.

Ås, May, 2014

Ida Roksvåg Byman

ABSTRACT

The aim of this study was to obtain further insight in family 19 chitinases by carrying out a kinetic and functional characterization of a bacterial family 19 chitinase from *Streptomyces coelicolor* A3(2). There are many family 19 chitinases, but it is still not quite clear what these enzymes do. More fundamental enzymology is needed to learn about the details of these enzymes. Calculating kinetic parameters like K_m and k_{cat} under various conditions and for various substrates can provide such details.

In the present study, Chitinase G from *S. coelicolor* A3(2) was expressed in a pETM11 vector and purified using immobilized-metal affinity chromatography. After method development to establish reliable quantitative analysis of reaction products, kinetic parameters were obtained from enzyme assays using natural soluble chitooligosaccharides as substrates. K_m and k_{cat} for $(GlcNAc)_3$, $(GlcNAc)_4$ and $(GlcNAc)_5$ were 4.9 (± 0.8) × 10^3 µM and 215 (± 21) s^{-1}, 5.6 (± 0.40) × 10^2 µM and 584 (± 14) s^{-1} and 5.3 (± 0.84) × 10^2 µM and 451 (± 24) s^{-1}, respectively. The similar K_m values of the tetramer and the pentamer indicate that the enzyme has only four substrate-binding subsites. In addition, enzyme assays were performed at pH 4 to 8 using $(GlcNAc)_4$ as substrate, which revealed minimal effect on the enzyme activity. Chitinase G activity towards other substrates than chitin was tested, including other polysaccharides, cell walls of some bacteria and a fungus, using size exclusion chromatography and MALDI-TOF mass spectrometry for product analysis. However, no novel activities were detected.

High K_m values obtained from enzyme assays indicate low affinity towards the substrates tested, even though high k_{cat} values may indicate that the main substrate target is chitin, or at least a β−1,4 glycosidic bond between two *N*-acetylglucosamines, after all. More research is needed to understand the biological roles of these enzymes.

SAMMENDRAG

Målet med dette studiet var å få større innsikt i en familie 19 kitinase ved å utføre en kinetisk og funksjonell karakterisering av en bakteriell familie 19 kitinase fra *Streptomyces coelicolor* A3(2). Det finnes mange familie 19 kitinaser, men det er fortsatt ikke helt klart hva disse enzymene gjør. Mer fundamental enzymologi trengs for å lære om detaljene i disse enzymene. Kalkulering av kinetiske parametere som K_m og k_{cat} under forskjellige forhold og for forskjellige substrater kan gi slike detaljer.

I dette studiet ble Kitinase G fra *S. coelicolor* A3(2) uttrykt i en pETM11 vektor, og renset ved å bruke immobilisert-metal affinitetskromatografi. Etter metodeutvikling for å etablere pålitelige kvantitative analyser av reaksjonsprodukter, ble kinetiske parametere kalkulert basert på enzymassayer hvor naturlige, løselige kitooligosakkarider ble brukt som substrat. K_m og k_{cat} for $(GlcNAc)_3$, $(GlcNAc)_4$ og $(GlcNAc)_5$ var henholdsvis 4.9 (± 0.8) × 10^3 µM og 215 (± 21) s^{-1}, 5.6 (± 0.40) × 10^2 µM og 584 (± 14) s^{-1} og 5.3 (± 0.84) × 10^2 µM og 451 (± 24) s^{-1}. Liknende K_m verdier for tetrameren og pentameren indikerer at enzymet kun har fire substratbindende seter. Det ble i tillegg utført enzym-assayer ved pH 4 til 8 ved bruk av $(GlcNAc)_4$ som substrat, noe som viste at pH hadde minimale effekter på enzymaktiviteten. Aktivitet mot andre substrater enn kitin ble også testet for Kitinase G, inkludert andre polysakkarider, celleveggen til noen bakterier og en sopp. Eksklusjonskromatografi og MALDI-TOF massespektrometri ble brukt til å analysere eventuelle produkter. Det ble imidlertid ikke oppdaget nye aktiviteter.

Høye K_m verdier kalkulert fra enzymassayene indikerer lav affinitet ovenfor de testede substratene, selv om høye k_{cat} verdier kan indikere at hovedsubstratet likevel kan være kitin, eller i det minste β-1,4 glykosidbindingene mellom to *N*-acetylglukosaminer. Mer forskning er nødvendig for å forstå de biologiske rollene til disse enzymene.

ABBREVIATIONS

BSA	Bovine Serum Albumin
CAZy	Carbohydrate-active enzymes
ChiC	Chitinase C from *Streptomyces griseus* HUT6037
ChiG	Chitinase G from *Streptomyces coelicolor* A3(2)
dH_2O	Sterilized milli-Q water
g	Gravitational acceleration
GH	Glycoside hydrolase
GlcNAc	*N*-acetylglucosamine
HPLC	High Performance Liquid Chromatography
LB	Luria-Bertani
MALDI-TOF	Matrix-assisted laser desorption/ionization – time of flight
MS	Mass Spectrometry
rpm	Rotations per minute
v/v	Volume/volume
w/v	Weight/volume

CONTENTS

1 INTRODUCTION

Chitinases are enzymes that degrade the polysaccharide chitin, a polymer of β−1,4 linked *N*-acetylglucosamine found in abundance in nature. Based on amino acid sequence, chitinases are divided into glycoside hydrolase (GH) family 18 and 19. Research on GH19 chitinases has not received as much attention as GH18 chitinases, and the roles of these enzymes are not completely understood. Furthermore, the enzymology of family 19 chitinases has been poorly studied. GH19 chitinases were originally thought to exclusively exist in higher plants, but have later been discovered in bacteria (Ohno et al., 1996) and a few other organisms. This thesis describes the characterization of a bacterial family 19 chitinase, and provides novel fundamental insight into this family of enzymes.

1.1 Carbohydrates

Carbohydrates are organic molecules that are present in all living organisms. The functions of carbohydrates include energy storage (e.g. starch in plants), structural roles (e.g. chitin in crustaceans, cellulose in plants) and signalling roles (e.g. protein glycosylation). In nature carbohydrates usually occur in the form of oligosaccharides and polysaccharides. The minimal unit of these molecules are monosaccharides, which are connected by glycosidic bonds between a hemiacetal group and a hydroxyl group of the respective saccharides. Polysaccharides have more than twenty monomers linked together (and oligomers have less), but the degree of polymerization varies and most polysaccharides consist of 200-3,000 units (Damodaran et al., 2008). A polymer consisting of different units is called a heteropolymer, whereas the term homopolymer is used if the units are all the same. In addition, the polysaccharides can be linear or branched, whereas the degree of branching may vary. Several types of monomers exist, and in addition, the carbon atom in the hemiacetal group of these monomers can accommodate two different steric configurations, named α and β. There are additionally different types of glycosidic linkages connecting the monomers. In total, these carbohydrates thus comprise a variety of molecular structures. Polysaccharides are found in abundance in nature, and have important biological roles as well as an increasing number of applications in the industry.

1.1.1 Chitin

Chitin is a linear homopolymer of *N*-acetylglucosamine units (GlcNAc) linked together by β-1,4 glycosidic bonds. Structurally, chitin resembles cellulose, except that there is an acetamido group attached to the second carbon atom in each monomer, whereas this position has a hydroxyl group in cellulose (Figure 1.1). Monomers are rotated 180º relative to each other in both polysaccharides. In nature chitin polymers most commonly form ordered crystalline microfibrils that are organized in a planar network (Muzzarelli, 2011). The spacing between the microfibrils in the network can accommodate substances such as pigments, inorganic compounds, sugars, proteins or glycoproteins (Muzzarelli, 2011).

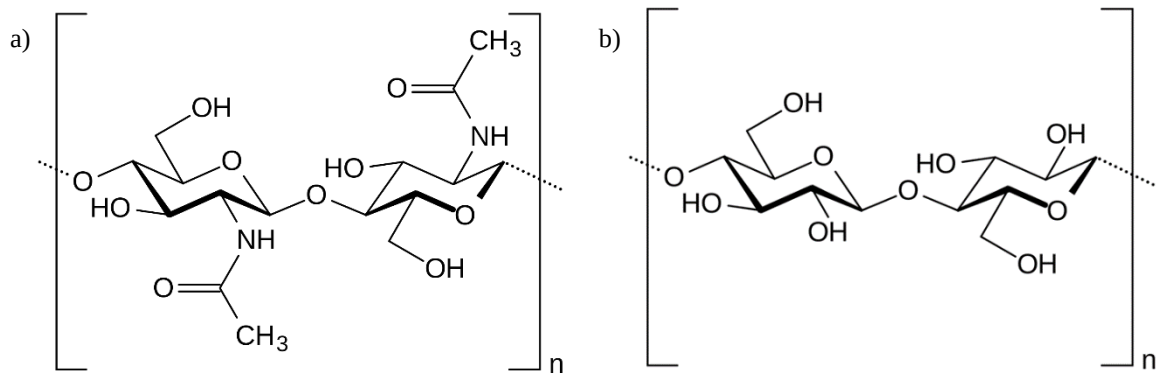

Figure 1.1. Repeating disaccharide units in chitin (a) and cellulose (b). Chitin consist of *N*-acetylglucosamine units linked together by β-1,4 glycosidic bonds. Cellulose is structural similar to chitin. The figure is adapted from http://en.wikipedia.org/wiki/Chitin.

Chitin is recalcitrant and insoluble in water, but deacetylated derivatives of chitin, called chitosan, are soluble in dilute acid solutions (Rinaudo, 2006). Chitin is known to function as a structural component in the cell wall of fungi and yeast and in the cuticle of arthropods (Rinaudo, 2006). The annual production of chitin is in the range of 10^{10}-10^{11} tons, making chitin the second most abundant biopolymer on earth next after cellulose (Gooday, 1990) .

In nature chitin occurs in three different allomorphs based on the orientation of the chains in the crystalline microfibrils. The most common variant is α-chitin where the adjacent chitin chains are organized antiparallel to one another in sheets (Minke and Blackwell, 1978). The chains are connected through a number of intra-sheet hydrogen bonds (Muzzarelli, 2011). In addition, there are some hydrogen bonds between the sheets which is unique to α-chitin and allows tight packing in microfibrils (Muzzarelli, 2011). The second most abundant allomorph is β-chitin where the polymer chains are organized in a parallel orientation, and linked together by hydrogen bonds (Gardner and Blackwell, 1975). In contrast to α-chitin, β-chitin does not form hydrogen bonds between sheets. This gives the latter chitin formation the property of swelling because of the extra hydroxyl groups that are free to make hydrogen bonds with water molecules (Muzzarelli, 2011). The third naturally occurring chitin allomorph is γ-chitin, where two parallel polysaccharide chains alternate with one anti-parallel chain. The existence of the γ-chitin variant is still disputed and it is thought to be very rare (Rinaudo, 2006). The three different allomorphs are thought to provide various structural properties, such as α-chitin giving more mechanical strength (e.g. in exoskeleton of crustaceans) and β-chitin and γ-chitin giving softer chitinous structures (e.g. in cocoons) (Merzendorfer and Zimoch, 2003).

1.2 Enzymatic degradation of chitin

The recalcitrance of chitin has forced the evolution of enzymes that can efficiently degrade this carbohydrate. Organisms produce enzymes acting on chitin, such as chitinases, for different reasons. For example, chitinases are needed in organisms containing chitin (e.g. crustaceans), because they need chitin-degrading enzymes for remodelling during growth. Further, chitinases are produced by higher plants, which use the enzymes to defend themselves against pathogenic attacks by degrading chitin in the cell walls of fungi and bacteria. In addition, the abundance of chitin in nature makes this carbohydrate an excellent source of carbon and nitrogen for microbes, some of which are indeed known to secrete many chitinases.

Enzymatic degradation of chitin can follow two different paths: a chitinolytic path or via chitosan. The chitinolytic process require direct hydrolysis of the β-1,4 glycosidic bonds between the GlcNAc units by chitinases (Beier & Bertilsson, 2013). Chitinolytic activity is also accomplished by the recently discovered lytic polysaccharide monooxygenases that work in synergy with the chitinases (Vaaje-Kolstad et al., 2010). Alternatively, chitin can be degraded by first being solubilized by deacetylation. This process is carried out by chitin deacetylases, and the derived substrate (chitosan) is hydrolysed by chitosanases.

1.2.1 Classification of carbohydrate-active enzymes

Carbohydrates play important roles in many biological processes, which has resulted in development of a large diversity of enzymes acting on these biomolecules. The different enzyme activities can be classified using several different criteria. The oldest method uses a nomenclature decided by the specific reactions that the enzyme catalyzes, according to recommendations by the international committee of biochemistry and molecular biology (IUBMB, 2013). Each enzyme is provided with an Enzyme Commission number based on their function on a specific substrate. This system works well when the substrates are small, but when classifying enzymes that act on polymers it is not adequate because these enzymes may act on related polymers as well as their main substrate target (IUBMB, 2013, Henrissat and Davies, 1997).

Polysaccharide-active enzymes can also be classified based on their mode of action, such as the ‘exo’ and ‘endo’ modes, indicating whether the enzyme is cutting at an end or somewhere within the chain of a polysaccharide, respectively (Henrissat and Davies, 1997). Either of these modes may be combined with ‘processivity’, meaning that the enzyme hydrolyses multiple bonds before releasing the substrate. The shape of the substrate binding region of the active site has been found to reflect the mode of action (Davies and Henrissat, 1995), and three different shapes are recognized. The pocket shape is typical for ‘exo’-enzymes, whereas ‘endo’-enzymes usually have a cleft shape. In ‘processive’ enzymes these clefts tend to be deeper and may even appear as tunnels (Figure 1.2). In addition, classification based on the mechanism of action has been suggested, where the anomeric configuration of the product is been considered (Sinnott, 1990).

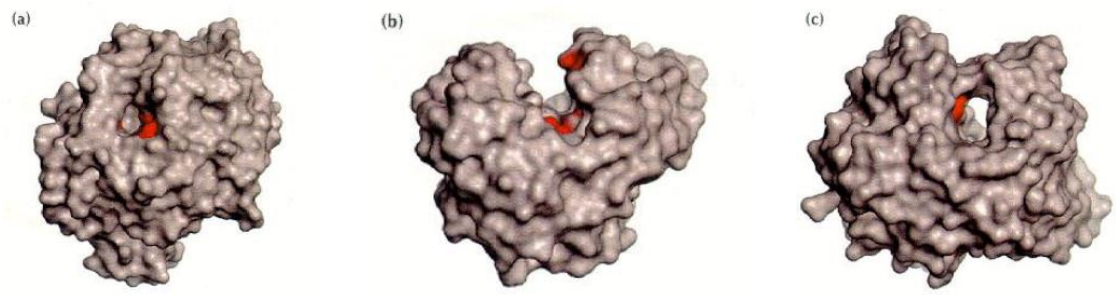

Figure 1.2. Typical shapes of exo, endo and processive glycoside hydrolasess. (a) Pocket shape of an exo-enzyme exemplified by glucoamylase from *Asperigillus awamori*. (PDB ID: 1GLM). (b) Cleft-shape in endo-enzymes exemplified by endoglucanase E2 from *Thermobifida fusca* (PDB: 2BOD). (c) Tunnel shape in processive enzymes exemplified by cellobiohydrolase II from *Thricoderma reseei*. (PDB: 415U). The picture is taken from (Davies and Henrissat, 1995).

Sequence and structure are related, therefore structural and mechanistic information of a protein can be derived from the amino acid sequence (Henrissat and Davies, 1997). This was the fundamental thought behind establishing a database for carbohydrate-active enzymes (CAZy) based on amino acid sequence. In the CAZy database, enzymes with structurally relevant degrees of sequence similarity, i.e. enzymes with conserved folds and active site geometries are grouped into families (Davies et al., 2005). The database currently covers five enzyme classes acting on carbohydrates and glycoconjugates by either synthesis, breakdown or modification. GHs hydrolyse glycosidic bonds between glycosides. Polysaccharide lyases do also cleave glycosidic bonds, but in a non-hydrolytic fashion. Carbohydrate esterases include enzymes that deacetylate carbohydrate esters and amides. Biosynthesis of carbohydrates is accomplished by glycosyltransferases which catalyse the formation of glycosidic bonds. A fifth enzyme class called auxiliary activities has recently been added the CAZy database, triggered by the discovery of the lytic polysaccharide monooxygenases. These enzymes act cooperatively with other carbohydrate-degrading enzymes, by making the substrate more accessible. In addition, non-catalytic carbohydrate-binding modules are associated with the CAZy enzymes and are thus described in the database. A binding module is a part of a larger protein and enhances catalytic activity by binding to the carbohydrate and directing the catalytic domain towards the substrate (Bueren, 2013). By comparing novel sequences with the CAZy database, classification of these sequences can easily be accomplished, which makes this database a practical tool for predicting enzyme activity and function.

1.2.2 Catalysis in glycoside hydrolases

The majority of the carbohydrate-active enzymes are GHs which hydrolyse glycosidic bonds. Enzymatic hydrolysis of a glycosidic bond requires a proton donor (i.e. catalytic acid) and a nucleophile/base. The distance between the proton donating residue and the nucleophilic/basic residue usually determines whether the mechanism results in retention or inversion of the anomeric configuration of the saccharide (Figure 1.3) (Davies and Henrissat, 1995). In the retaining mechanism, the catalytic acid donates its proton to the oxygen in the glycosidic bond, while a residue in close enough distance (~ 5.5 Å between the residues) performs a nucleophilic attack on the anomeric carbon in the saccharide molecule, promoting leaving group departure and creating a covalent bond between the nucleophile and the anomeric carbon (Koshland, 1953). In the second step of this "double displacement mechanism", the catalytic acid acts as a base that polarizes a water molecule that performs a nucleophilic attack on the anomeric carbon in the intermediate enzyme-substrate complex. Thus, the configuration of the anomeric carbon atom is retained; i.e. the stereochemistry of the resulting reducing end of the product is identical to that in the former glycosidic linkage.

If the distance between the two crucial residues is approximately 10 Å the reaction happens in one step, with the nucleophilic attack being performed by a water molecule which has been activated by the catalytic base in the enzyme (Koshland, 1953). In this inverting mechanism, the catalytic acid has the same function as in the retaining mechanism. The result of the inverting mechanism is a product with the opposite configuration of the anomeric carbon than the internal linkages of the substrate. Ultimately, whether the stereochemistry of the anomeric carbon is retained or inverted is dependent on which side of the saccharide plan the water mediated nucleophilic attack is performed.

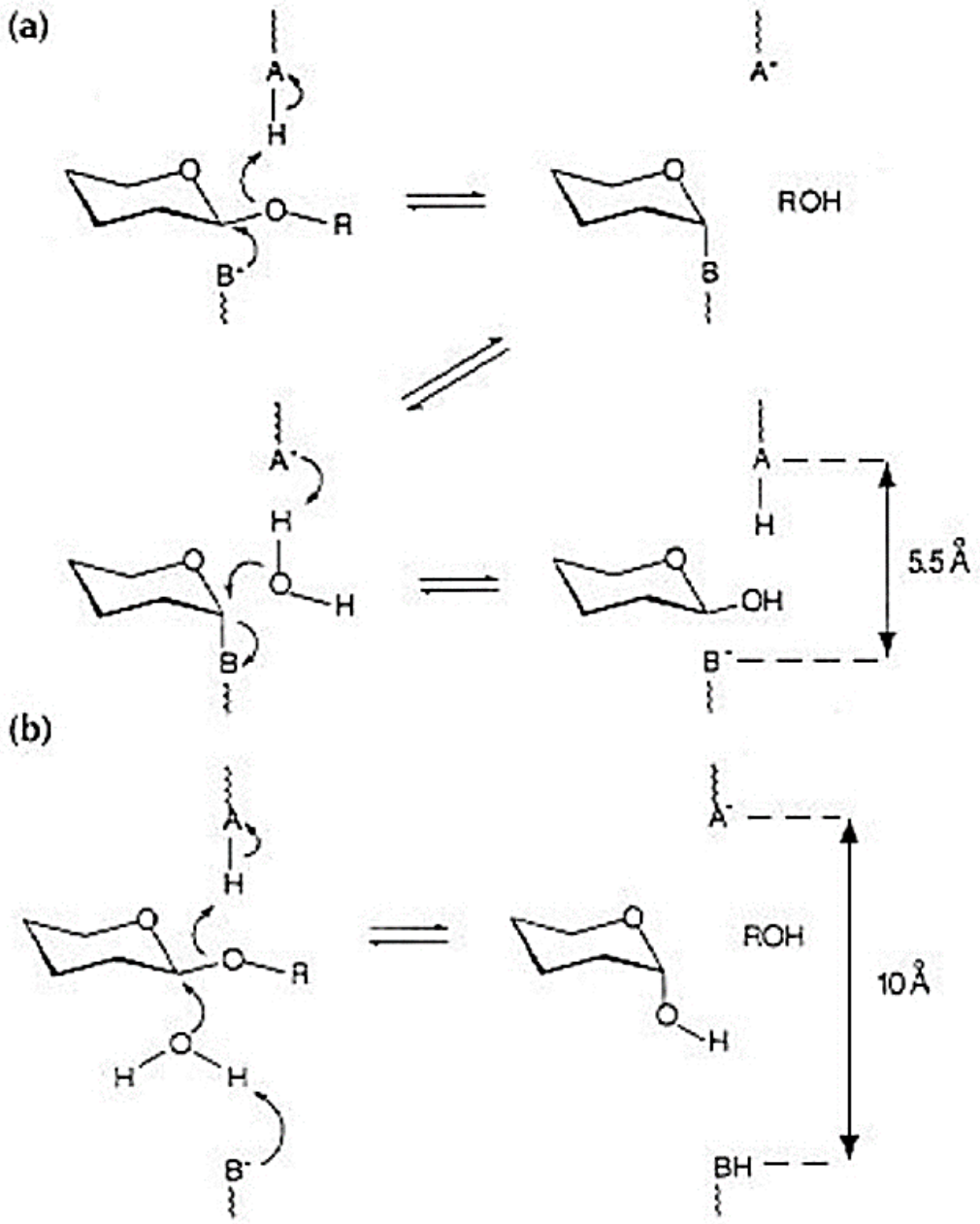

Figure 1.3. The catalytic mechanisms of glycoside hydrolases. (a) Retaining mechanism. The catalytic acid (-AH) donates its proton to the glycosidic bond, while a nucleophilic attack is performed on the anomeric carbon by a nucleophilic residue ($-B^-$). The next step involves a nucleophilic attack on the anomeric carbon by a water molecule that is activated by the deprotonated catalytic acid now acting as a base. **(b) Inverting mechanism.** The catalytic acid (-AH) donates its proton to the glycosidic bond as in the retaining mechanism, but this time nucleophilic attack on the anomeric carbon is performed by a water molecule activated by a basic residue ($-B^-$). This picture is taken from G. Davies & Henrissat (1995).

1.2.3 Chitinases

Based on amino acid sequence, chitinases belong to glycoside hydrolase families 18 and 19 (Henrissat and Davies, 1997). The catalytic domain of GH18 chitinases consist of a $(\beta/\alpha)_8$ barrel fold (Figure 1.4) and these enzymes use the retaining mechanism when hydrolysing their substrate. Family 19 chitinases have a catalytic domain with a high α-helical content and uses the inverting mechanism as their mechanism of action. In contrast to family 19 chitinases, family 18 chitinases are found in many different organisms, including bacteria, higher plants, animals, viruses and fungi, and are among the chitinolytic enzymes studied the best (Hoell et al., 2010). Family 19 chitinases are discussed in more detail below.

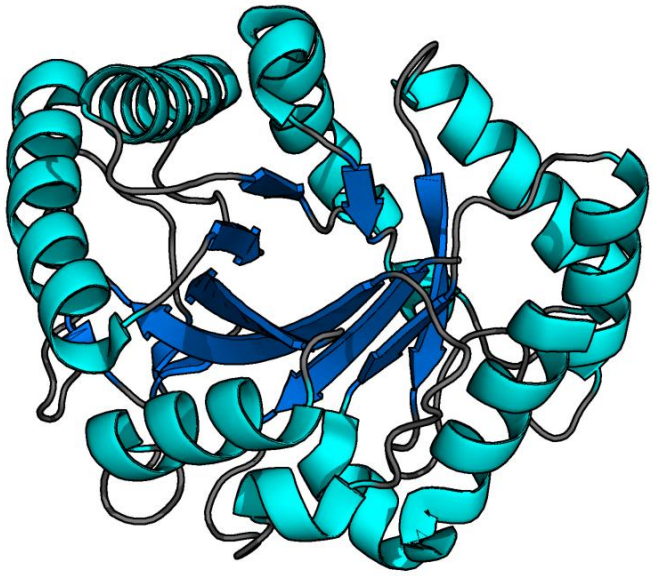

Figure 1.4. Structure of the catalytic domain of a GH18 chitinase. The cartoon representation is showing the $(\beta/\alpha)_8$ barrel fold exemplified with a family 18 chitinase from *Crocus vernus* (PDB: 3SIM). α-helices are coloured cyan, and β -strands are coloured marine. The picture was generated using Pymol (DeLano, 2002).

1.3 Family 19 chitinases

Family 19 chitinases were originally thought to exclusively exist in higher plants, but the discovery of Chitinase C (ChiC) in the *Actinobacterium Streptomyces griseus* HUT6037 (Ohno et al., 1996) revealed that chitinases within this family also could be found elsewhere. Since then, GH19 chitinases have been found in other bacteria and a few other organisms. A phylogenetic study showed that GH19 chitinases are mainly distributed in higher plants,

actinobacteria and purple bacteria (Prakash et al., 2010). Another phylogenetic study put forward the theory that GH19 chitinases in bacteria are acquired from higher plants by horizontal gene transfer (Watanabe et al., 1999). Furthermore, phylogenetic studies of actinobacteria and an analysis of the general occurrence of GH19 chitinases in *Streptomyces* spp. suggest that family 19 chitinase genes were acquired from a *Streptomyces* ancestor and spread to other actinobacteria by horizontal gene transfer (Kawase et al., 2004).

1.3.1 GH19 chitinase structures

Plant chitinases have been divided into five classes based on their primary structure, independent on the glycoside hydrolase classification (Collinge et al., 1993). Family 19 chitinases belongs to class I, II and IV. Class I and IV are multidomain chitinases with a cystein-rich N-terminal binding domain and a C-terminal catalytic domain connected through a linker peptide. Due to some deletions in the amino acid sequence, class IV enzymes are smaller than class I enzymes in both the binding and the catalytic domain. Class II enzymes only consist of a catalytic domain. As more crystal structures of the catalytic domains of GH19 chitinases have been solved, the catalytic domains have been subdivided into two types, currently termed “loopful” and “loopless” (see Figure 1.5).

The first known structure of a GH19 chitinase was reported for an enzyme purified from *Hordeum vulgare* (barley) seeds (Hart et al., 1993). A structural comparison between the barley enzyme and lysozymes showed that the secondary structures in the active site regions were similar (John Hart et al., 1995, Holm and Sander, 1994). Lysozymes are known to degrade peptidoglycans, resulting in breakdown of some bacterial cell walls. Some lysozymes also act on partially deacetylated chitin. The catalytic domains of family 19 chitinases also show structural resemblance to family GH46 chitosanases (Monzingo et al., 1996). The solved structure of a family 19 chitinase from jack beans did also show structural similarity to lysozymes, but the architecture of the active site suggested a different catalytic mechanism from the lysozymes which uses the retaining mechanism (Hahn et al., 2000).

In 2006 the structures of two bacterial family 19 chitinases were solved, revealing the first "loopless" GH19 chitinases. The structure of ChiC from *S. griseus* HUT6037 (Kezuka et al., 2006) and the structure of ChiG from *S. coelicolor* A3(2) (Hoell et al., 2006) were lacking loops at both ends of the substrate-binding cleft compared to the former structures reported for family 19 chitinases (see Figure 1.5). Plant chitinases purified and crystillized from *Picea abies* (Norway spruce) and *Bryum coronatum* (moss) are also reported to be "loopless" (Ubhayasekera et al., 2009, Taira et al., 2011).

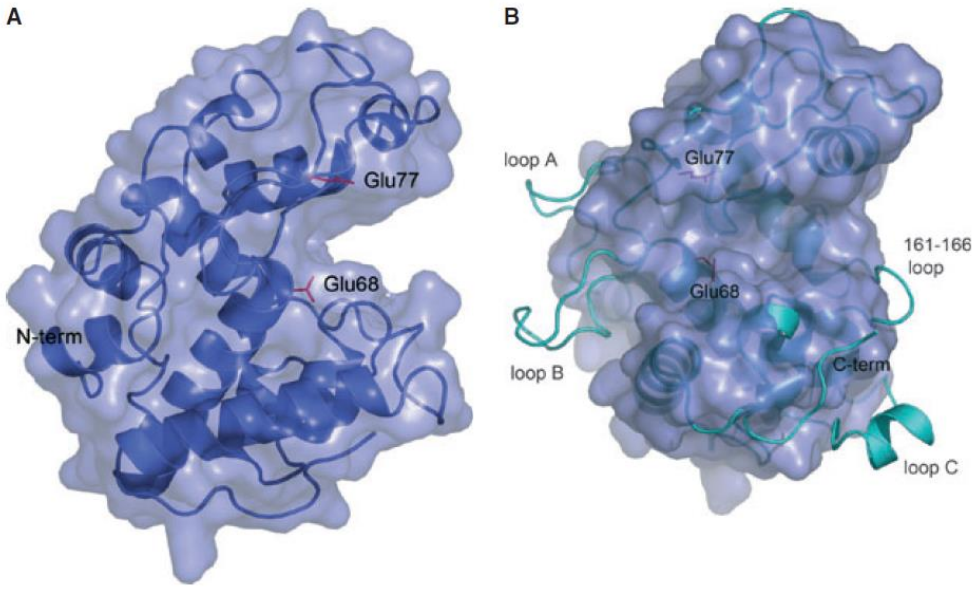

Figure 1.5 Structural comparison of a "loopless" and a " loopful" family 19 chitinase. (A) The cartoon representation is showing the architecture of the "loopless" ChiG with transparent surface showing the overall shape. Catalytic residues are shown in sticks and labeled (PDB: 2CJL). (B) Superimposed structure of ChiG (shown in surface reprecentation) and the "loopful" barley chitinase (shown in cartoon) (PDB: 2BAA). The figure is taken from (Hoell et al., 2006).

The crystal structure of a "loopful" family 19 chitinase from *Carica papaya* was solved with two GlcNAc entities located in the active site of the enzyme, at subsites -2 and +1 (Huet et al., 2008). In 2013 complete subsite mapping of another "loopful" family 19 chitinase from *Secale cereal* (rye) seeds was reported based on its crystal structure in complex with two $(GlcNAc)_4$ molecules (Ohnuma et al., 2013). The chitin tetrasaccharides occupied subsite -4 to -1 and +1 to +4, respectively. From combining the structural data with studies on the degradation of chitooligosaccharides, the authors concluded that this loopful enzyme has eight subsites, and that GlcNAc binds strongly to residues at subsite -2, -1 and +1. Very recently the crystal structure of an inactive mutant (E61A) of a "loopless" GH19 chitinase from moss was solved in complex with $(GlcNAc)_4$ binding to subsites -2 to +2 (Ohnuma et al., 2014).

1.3.2 Catalysis by GH19 chitinases

The catalytic mechanism for GH19 chitinases has previously been poorly understood because of the lack of structures of enzyme-substrate complexes. Based on molecular dynamics simulations using the crystal structure of barley chitinase an inverting mechanism was proposed (Brameld and Goddard, 1998). Crystal structures reported after have been consistent with this suggested hydrolysis mechanism. The very recently reported crystal structure of the E61A mutant of the GH19 chitinase (BcChi-A) from *B. coronatum* in complex with $(GlcNAc)_4$ validates the inverting mechanism for family 19 chitinases (Ohnuma et al., 2014). These recent data are in accordance with the mechanism described by Brameld and Goddard (1998). Both the catalytic acid and the catalytic base are glutamates, within expected distances for the inverting mechanism to occur. A serine residue fixes the position of the nucleophilic water molecule through a hydrogen bond (Figure 1.6). This novel structure showed that the glycoside linkage between subsite -1 and +1 is twisted, which possibly can lower the activation energy for hydrolysis.

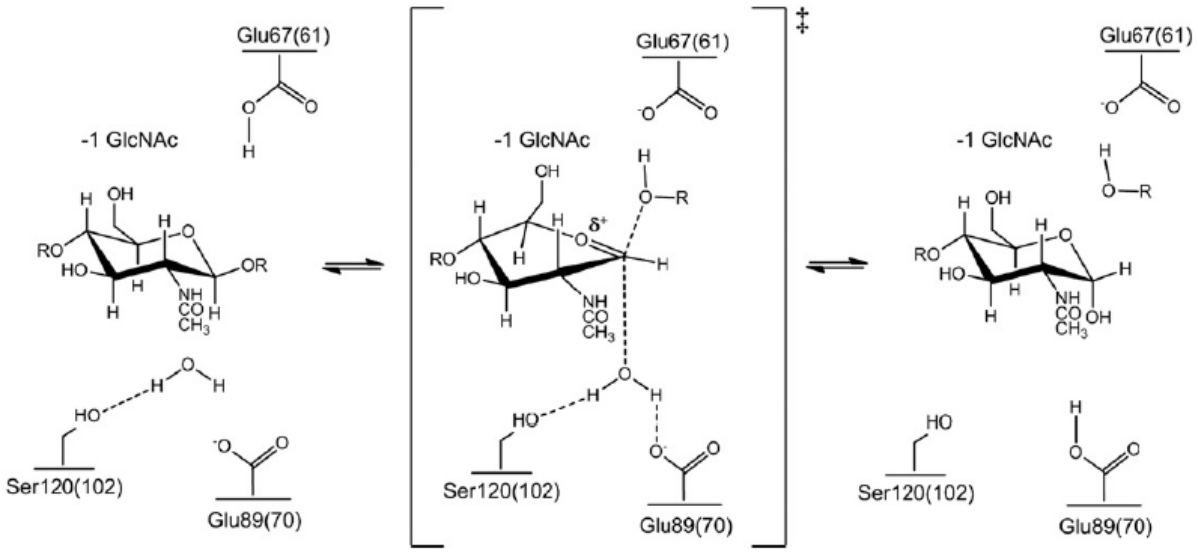

Figur 1.6. Inverting mechanism in GH19 chitinases as described by Ohnuma et al., (2014). The residue numbering applies to the barley and jack bean chitinases with the numbering of BcChi-A in parenthesis. Glu67(61) donates a proton to the oxygen in the glycosidic bond. Ser120 (102) fixes the position of a water molecule that is activated by Glu89 (70) and subsequently performs a nucleophilic attack of the anomeric carbon atom. This picture is taken from (Ohnuma et al., 2014)

1.3.3 Biological function of GH19 chitinases

The biological function of family 19 chitinases in general is not clear. In plants GH19 chitinases are thought to be a part of the defence system against pathogenic fungi (Brogue et al., 1991), suggesting a role in chitin degradation. However, these enzymes seem also involved in tolerance for environmental stresses such as freezing (Pihakaski-Maunsbach et al., 2001), high salinity and drought (Hong and Hwang, 2002). In addition, it has been shown that a GH19 encoding gene is important in normal plant growth (Zhong et al., 2002). In bacteria, activity of a family 19 chitinase towards chitinous substrates was reported to be higher than for the family 18 chitinases in the same organism (Watanabe et al., 1999). In addition, antifungal activiy is shown for certain family 19 chitinases found in *Streptomyces* spp. (Kawase et al., 2006, Watanabe et al., 1999), suggesting that these chitinases are adventadgeous in the interaction between fungi and *Streptomyces* spp. The reasearch on GH19 chitinases are deficient, and one reason for the current uncertainty as to the biological function of GH19 chitinases is the lack of solid kinetic data and activity studies on other substrates than chitin. Clearly, more research on this topic is needed.

1.4 Chitinase G

Chitinase G (ChiG) is a family GH19 chitinase found in the *Actinobacterium Streptomyces coelicolor* A3(2). Within the bacterial domain, the actinobacteria comprise one of the largest phyla, and these bacteria show a wide variety of morphologies and functionalities (Ventura et al., 2007). Actinobacteria are gram-positives, and they have adopted very different lifestyles (e.g. soil inhabitants or pathogens). One of the soil-living bacterial families of the phylum are the *Streptomycetaceae* that are responsible for breakdown of organic materials, including cellulose and chitin. *Streptomyces* spp. are considered to be the major bacterial producers of chitinases, and have a high multiplicity of chitinase genes (Saito et al., 1999). The catalytic domains of family 19 chitinases in *Streptomyces* spp. belong to class IV in the plant classification system described above (Watanabe et al., 1999). *S. coelicolor* A3(2) is commonly used as a model organism, and the genome sequence of this bacterium was determined more than ten years ago (Bentley et al., 2002). The genome contains eleven GH18 chitinase encoding genes and two GH19 chitinase genes (*chiG* and *chiF*).

Studies of secretion or expression of chitinases from *S. coelicolor* are inconclusive as to the role of these enzymes. A recent study investigated the secretome and transcriptome of the close relative *S. sirexAA-E* (Takasuka et al., 2013). Here expression of the ChiG homologue (SACTE_0081) and a second GH19 chitinase (SACT_3064) was observed to be highly upregulated when the bacterium was grown on chitin as a carbon source. It should be noted, however, that the GH19 enzymes also were upregulated when plant cell wall polysaccharides were used as carbons sources. Another study had previously reported that *ChiG* was not upregulated when grown on colloidal chitin, even though *ChiF* was upregulated along with some of the family 18 chitinases (Saito et al., 2000). A third study did not include ChiG, but also showed expression of *ChiF* in the presence of chitin (Kawase et al., 2006).

1.4.1 Structure of Chitinase G

As discussed above, ChiG is a "loopless" GH19 chitinase (Figure 1.5). The enzyme surface reveals a cleft-shape, typical for the endo-acting enzymes. The two catalytic residues, Glu68 and Glu77, are located within the cleft. ChiG only consists of a catalytic domain, and has no substrate/chitin binding domain.

The crystal structure of ChiG was solved without substrate (Figure 1.5). However, in a mutational study Hoell et al. (2009) attempted to map the roles of residues involved in substrate-binding in ChiG. This mutational study showed that Trp112, Asn115, Tyr148, Tyr86, His67 and Gln109 are important in binding the substrate and thereby important for catalytic efficiency (Fig. 1.6). In addition, Asn178, Glu182 and Arg194 were found to be important for activity, probably by creating the correct electrostatic environment for the catalytic acid, Glu68. The recently described crystal structure of BcChi-A (Ohnuma et al., 2014) provides further insight in to enzyme-substrate interactions. Interestingly, this study included a structural superimposition with ChiG, revealing a high root-mean-square deviation of 1.334 Å which probably is due to (substrate-free) ChiG being in a more open conformation.

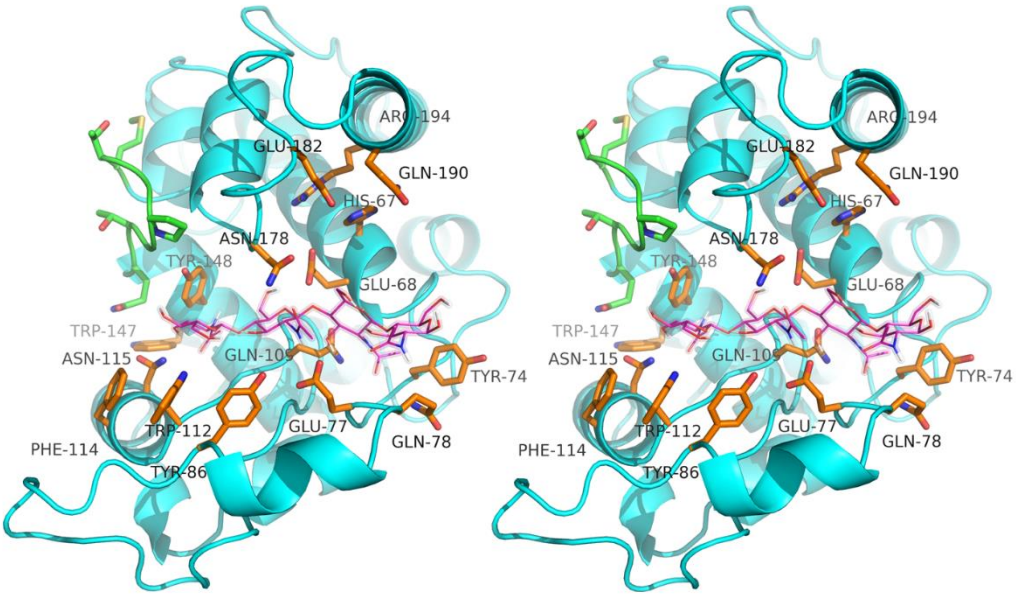

Figure 1.6. Enzyme-substrate interactions in the ChiG-$(GlcNAc)_4$ complex. Stereo image of the ChiG active site. The protein main chain is shown as a cyan cartoon, and the side chains of residues that have been subjected to mutagenesis are shown in orange stick representation. Loop IV is coloured green and its side chains are shown in green stick representation. The docked (GlcNAc)4 is shown in magenta line representation. All side chain and ligand oxygen and nitrogen atoms are coloured red and blue, respectively. Figure and ligand is taken from (Hoell, 2009)

1.5 Enzyme kinetics

The purpose of an enzyme is to catalyse a chemical reaction, meaning that it makes a reaction reach its equilibrium faster. Several tricks are used by the enzymes to make this happen, and lowering the activation energy of the reaction by stabilizing the transition state is the most common explanation for enzymatic action. Several factors affect the reaction rate; pH, ionic strength, temperature and the concentrations of enzyme, substrate, products, inhibitors and activators (Segel, 1993). Enzyme kinetics is used for analysis of these catalysed reactions, and can give useful insight concerning the enzyme mechanism and the architecture of the catalytic centre (Segel, 1993).

A model to account for the dynamics of enzymes, was proposed by the scientists Michaelis and Menten in the early 20th century (Segel, 1993). Some important assumptions were made when making the model. First, it is assumed that substrate (S) and enzyme (E) form a complex (ES) rapidly, and that these three components are in equilibrium (Eq. 1). In other words, the dissociation of the complex to substrate and enzyme is faster than product

formation. In addition, the substrate concentration has to be much higher than the enzyme concentration, so that formation of the ES-complex does not affect the substrate concentration. The velocity has to be measured at an early stage, so that the rate constant from product to the ES-complex is negligible. The Michaelis-Menten equation is based on unireactant enzymes.

$$E + S \underset{k_{-1}}{\overset{k_1}{\rightleftharpoons}} ES \xrightarrow{k_2} E + P \qquad \text{(Eq. 1)}$$

These assumptions essentially imply that catalysis happens under steady state conditions, i.e. conditions at which the enzyme, substrate and ES-complex concentrations are constant over a period of time (Figure 1.7). The notion that the rate of formation of ES (k_1) then is equal to the rate of breakdown of the complex to release either substrate or product ($k_{-1} + k_2$) is at the very core of the Michaelis-Menten approach, hence the term steady-state kinetics.

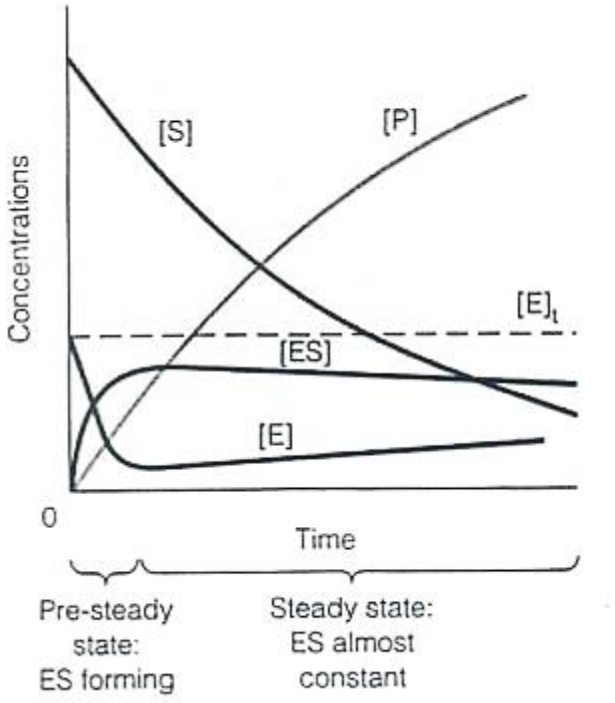

Figure 1.7. Steady-state kinetics. Picture captured from: http://web.campbell.edu/faculty/nemecz/323_lect/enzymes/enz_chapter.html

The Michaelis-Menten equation (Eq. 2) is a mathematical expression that provides some useful parameters when doing enzyme characterization. K_m (Eq 3) is the dissociation constant of the enzyme-substrate-complex (also called the Michaelis-Menten constant), and is often considered indicative of the enzyme's affinity for the substrate. The numerical definition of K_m is "the substrate concentration which gives half the maximum rate" (Engel, 1977). A high K_m means that high substrate concentrations are needed to achieve maximum rate of the reaction (V_{max}), and suggests low affinity for the substrate. Another useful parameter is k_{cat}, which describes the amount of substrate converted to product per amount of enzyme and time. In unireactant enzymes k_{cat} is the same as k_2 in Eq. 1. k_{cat} is related to V_{max} according to Eq 4.

$$v = \frac{V_{max}\ [S]}{[S] + K_m} \qquad \text{(Eq. 2)}$$

$$K_m = \frac{k_{-1} + k_2}{k_1} \qquad \text{(Eq. 3)}$$

$$k_{cat} = \frac{V_{max}}{[E]_0} \qquad \text{(Eq. 4)}$$

The Michaelis-Menten equation (Eq. 2) describes the relationship between the substrate concentration ([S]) and the reaction rate (V) and yields also a hyperbolic curve (Figure 1.8). Both the rates of substrate degradation and product formation can be used to determine reaction rates.

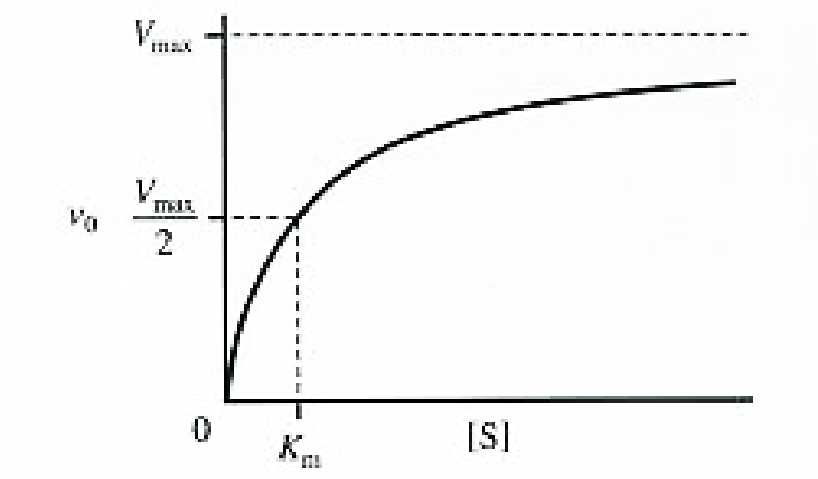

Figure 1.8. The Michaelis-Menten plot.
Picture captured from: http://web.campbell.edu/faculty/nemecz/323_lect/enzymes/enz_chapter.html

1.6 Purpose of this study

Research on GH19 chitinases has not received as much attention as research on GH18 chitinases and more fundamental enzymology is needed to shed light on the function of these enzymes. The aim of this study is to contribute to GH19 research by studying a bacterial family GH19 chitinase. New structure information is now available and this combined with new kinetic data could possibly give a deeper understanding of substrate-binding in ChiG generating knowledge possibly extending to family 19 chitinases in general.

The experimental work done to achieve this goal included expression of ChiG in *Escherichia coli*, enzyme purification by immobilized-metal affinity chromatography, and detailed kinetic characterization using the substrates $(GlcNAc)_3$, $(GlcNAc)_4$ and $(GlcNAc)_5$. Kinetic characterization was also performed at pH 4 to 8, using the $(GlcNAc)_4$ as substrate, in order to study the pH-dependency of activity. Furthermore, the activity of ChiG towards an array of other potential substrates, including various polysaccharides, peptidoglycan, bacterial cell walls and a fungus was analysed.

2 MATERIALS

2.1 Instruments

Instruments used in this study are listed in Table 2.1.

Table 2.1 Instruments used in this thesis and their suppliers.

Instrument	Supplier
BioLogic LP chromatographic system	BioRad
Spectrophotometer: Biophotometer	Eppendorf
Cell Density Meter: CO8000	WPA biowave
Centrifuges:	
Avanti ™ J-25 with JA-10 and JA-25.50 rotor	Beckman Coulter
Centrifuge 5430 R	Eppendorf
Centrifuge 5418 R	Eppendorf
FastPrep®-24	MP Biomedicals
Gel Doc™ EZ Imager	BioRad
Incubation shakers:	
Minitron	INFORS HT
Multitron	INFORS HT
ThermoMixer C	Eppendorf
Incubator cabinets	Termarks
Ultraflex TOF/TOF MS	Bruker Daltonics
pH-meter: 827 pH lab	Metrohm
Power Pac 300	BioRad
Rotator-mixer: Multi RS-60	BIOSAN
Sonicator: Vibracell	Sonics
Laminar flow bench, AV-100	TELSTAR
UHPLC: UltiMate 3000	DIONEX
Waterbath	Stuart/Julabo

2.2 Chemicals

Chemicals used in this study are listed in table 2.2.

Table 2.2. Chemicals used in this study and their suppliers.

Chemical	Supplier
2,5-dihydroxybenzoic acid, DHB	VWR
Acetonitrile	VWR
Agar-agar	Merck
Alginate	FMC BioPolymer
Arabinoxylan from wheat	Megazyme
Bacto™ Tryptone	Becton, Dickinson and Co
Bacto™ Yeast Extract	Becton, Dickinson and Co
Benchmark ladder	Life (Novex)
Beta glucan from barley	Megazyme
BHI media	Oxoid
Bis-Tris	Sigma
Cellulose monoacetate	Bjørge Westereng
D(+)-Saccharose	VWR
Di-Acetyl chitobiose	Megazyme
Di-Sodium hydrogen phosphate dihydrate	Merck
Difco™ potato dextrose broth	Becton, Dickinson and Co
Ethanol, 96 %	VWR
Glucose 20% (w/v)	Geir Mathiesen
Glycerol, 85% (v/v)	Merck
GM17 Broth	OXOID
Guar galactomannan	Megazyme
Hexa-Acetyl chitohexaose	Megazyme
Hydrochloric acid, HCl	Merck
Imidazole	Sigma
Isopropanol	Vinmonopolet A/S
Isopropyl β-D-1-thiogalactopyranoside, IPTG	VWR
Kanamycin	Sigma-Aldrich

Konjac glucomannan	Megazyme
Lichenan from Icelandic moss	Megazyme
Locus bean gum galactomannan	H. Stålbrand
Magnesium chloride, $MgCl_2$	Aldrich
MRS broth	VWR
Ni-NTA beads	Qiagen
NuPAGE® 10x Sample Reducing Agent	Life (Novex)
NuPAGE® 4x LDS Sample buffer	Invitrogen
Pectin	Københavns pektinfabrik
Penta-Acetyl chitopentaose	Megazyme
Peptidoglycan	In house-made by Daniel Straume
Phenylmethanesulfonylfluoride, PMSF	Sigma-Aldrich
Potassium chloride	Merck
Potassium dihydrogen phosphate, KH_2PO_4	Alfa Aesar
Potato extract	Fluka
Protein Assay dye reagent	BioRad
Purified BSA 100x	New England BioLabs inc.
Sodium Chloride, NaCl	Merck
Sodium hydroxide, NaOH	Merck
Sulfuric acid, H_2SO_4	Sigma-Aldrich
Tetra-Acetyl chitotetraose	Megazyme
TGS buffer(10X TGS)	BioRad
Titriplex® III, EDTA	Merck
Tri-Acetyl chitotriose	Megazyme
Trizma® base	Sigma-Aldrich
Xanthan gum in 5 mM $NaHPO_4$	Bjørge Westereng
Xylan from Aspen	Bjørge Westereng

2.3 Bacterial strains

Bacterial strains used in this study are listed in table 2.3.

Table 2.3. Bacterial strains used in this thesis and their suppliers.

Bacteria	**Supplier**
Escherichia coli, BL21 Star (DE3)/pETM11[1)]	I. Hoell (Hoell et al., 2006)
Lactobacillus plantanum WCFS1	G. Mathiesen
Endococcus feacalis V583	G. Mathiesen
Lactococcus lactis IL1403	G. Mathiesen

[1)] Strain for production of ChiG.

2.4 Enzymes

Enzymes used in this study are listed in table 2.4.

Table 2.4. Enzymes used in this thesis and their suppliers.

Enzyme	**Supplier**
Bovine Serum Albumin (BSA)	New England BioLabs
DNase I	Sigma
Lysozyme	Sigma
Mutanolysin	Sigma
RNase A	New England BioLabs
RNase B	New England BioLabs
Trypsin	Fluka

2.5 Fungi

Oscar Bengtsson provided the fungus used in this study, *Trichoderma reesei* /QM6a.

2.6 Software

Software used in this thesis are listed in table 2.6.

Listing table 2.6. Software used in this thesis and their application.

Software	Application
BioLogic LP data view	Used with the BioLogic LP chromatographic system.
Dionex™ Chromeleon™ 7.2 CDS	Used with the Ultimate 3000 HPLC
FlexAnalyzer	Data analysis for MALDI-TOF MS
FlexControl	Used with the Ultraflex TOF/TOF.
GraphPad Prism	Biostatistics and curve fitting.
Image lab	Captures and analyzes digital images of gels.
PROPKA	Calculations of pK_a values.

3 METHODS

3.1 Cultivation and storage of bacteria

3.1.1 Cultivation of bacteria

Bacteria were cultivated in various media and temperatures to achieve optimum growth.

Materials:

- Luria-Bertani broth (LB) medium
  - 10 g Bacto™ Tryptone
  - 10 g Bacto™ Yeast Extract
  - 5 g Sodium Chloride, NaCl

  The materials were dissolved in sterile milli-Q water (dH_2O) to a final volume of 1 litre and autoclaved at 121 ºC for 15 minutes.
- Brain-Heart-Infusion medium
  - 37 g BHI

  BHI broth was dissolved in dH_2O to a final volume of 1 litre and autoclaved at 121 º C for 15 minutes.
- De Man, Rogosa, Sharpie medium
  - 55.2 g MRS broth powder

  MRS broth powder was dissolved in dH_2O to a final volume of 1 litre and autoclaved at 121 ºC for 15 minutes.
- Growth medium 17
  - 9.3125 g GM17 Broth
  - Glucose, 20% (w/v)

  GM17 broth was dissolved in 250 mL dH_2O and autoclaved at 121 ºC for 15 minutes. Glucose was added to a final concentration of 0.4 % (v/v) before use.
- 50 mg/mL kanamycin (in dH_2O)
- Laminar Flow bench, AV-100
- Shaking incubator, Minitron
- Incubator, Bacteriology Cabinet

Procedure:
Cultivation of BL21 Star® *Escherichia coli* cells was done overnight in LB medium at 37 ºC and 200 rpm in a Minitron shaking incubator. The *E.coli* cells contained a pETM11 vector with an antibiotic resistance gene, and the inserted *ChiG* gene. To prevent *E.coli* cells without *ChiG* (and other potentially contaminating bacteria) from growing, 5 µL of the antibiotic kanamycin (50 mg/ml) was added per 5 mL LB medium.

Lactobacillus plantanum was grown overnight in De Man, Rogosa, Sharpie medium at 37ºC without shaking, using a Termaks incubator cabinet.

Enterococcus feacalis was grown overnight in Brain-Heart-Infusion medium at 30 ºC without shaking, using a Termaks incubator cabinet.

Lactococcus lactis was grown overnight in Growth Medium 17 at 30 ºC without shaking, using a Termaks incubator cabinet.

Microbiology work was conducted in a AV-100 laminar flow bench.

3.1.2 Long-term storage of bacteria

Materials:

- Selected bacterial culture
- Glycerol, 85 % (v/v)
- Cryo tubes (Gentaur)
- Laminar Flow bench, AV-100

Procedure:
A glycerol stock was made of *E. coli* BL21 Star™/pETM11-*ChiG*. To make a glycerol stock, cells were first cultivated according to section 3.1.1. Then, 700 µL bacterial culture and 300 µL glycerol were mixed in a cryo tube and stored at -80 ºC. Glycerol is added to avoid disruption on the cell membrane during storage at such low temperatures. The work was conducted on a AV-100 laminar flow bench.

3.2 Expression and purification of proteins

3.2.1 Expression of *ChiG*

Expression of *chiG* was accomplished by cultivation and induction of *E. coli* containing the pETM11 vector fused with the *ChiG* gene.

Materials:

- BL21 Star® *E.coli* cells containing *chiG*
- LB medium (see section 3.1.1)
- 50 mg/mL kanamycin (in dH_2O)
- 1 M IPTG
- Shaking incubator, Multitron
- Cell Density Meter, CO8000
- Shake flask, 2 L (Sigma)

Procedure:
Growth medium was prepared by combining 1.2 L LB medium and 1.2 mL 50 mg/mL kanamycin in 2 litre shake flasks. The culture medium was inoculated with 12 mL overnight grown bacterial culture (see section 3.1.1) of BL21 Star® *E.coli* cells containing pETM11-*ChiG*. The culture was incubated in a shaking incubator at 37 ºC and 200 rpm until the optical density reached 0.6. To induce the expression of the *chiG* gene, IPTG was added to a final concentration of 0.4 mM. Incubation of the bacterial culture at 30ºC and 200 rpm was then continued for four hours, followed by harvesting of the bacterial cells by centrifugation (see section 3.2.2).

3.2.2 Preparation of periplasmic extract

Materials:

- Culture of *E. coli* cells expressing *chiG*
- Spheroplast buffer
    - 30 mL 1 M TrisHCl pH 8
    - 51.3 g Saccharose
    - 300 µL 0.5 M EDTA pH 8
    - 600 µL 50 mM PSMF

  The components were mixed in dH_2O to a total volume of 300 mL.
- 20 mM $MgCl_2$
- 50 mM PSMF
- 0.22 µm sterile filter
- 50 mL syringe
- Centrifuge, Beckman Coulter Avanti ™ J-25 with JA-10 and JA-25.50 rotor
- Centrifuge tubes, 50 mL and 250 mL
- Cellstar® tube (Greiner Bio-One), 50 mL

Procedure:

To prepare the periplasmic extract, 600 mL bacterial culture containing expressed *chiG* was distributed in 250 mL centrifuge tubes, and centrifuged with a JA-10 rotor for 10 minutes at 7168 × *g* and 4 ºC. The supernatant was discarded and the cell-containing pellet was resuspended in 60 mL ice-cold spheroplast buffer. The cell suspension was transferred to 50 mL centrifuge tubes and centrifuged for 10 minutes at 7741 × *g* and 4 ºC in a JA-25.50 rotor (this rotor was utilized through rest of this procedure). The pellet was subsequently incubated at room temperature for 10 minutes, before resuspension in 50 mL ice-cold dH_2O, incubation on ice for 45 seconds and, finally, addition of 2.5 mL 20 mM $MgCl_2$. One last centrifugation was then done for 10 minutes at 17,418 × *g* and 4 ºC. The supernatant (containing the periplasmic proteins) was passed through a 0.22 µm sterile filter into a sterile 50 mL Cellstar® tube and 2 µL 50 mM PSMF was added per 1 mL extract to prevent proteases from destroying the overexpressed protein. The periplasmic extract was stored at 4°C until use.

3.2.3 Sonication of lysed cells

Materials:

- Culture of *E. coli* cells expressing *chiG*
- 20 mM TrisHCl pH 8.0
    - 2.428 g Trisbase
    - 6 M HCl

      Trisbase was dissolved in 90 mL dH_2O, and titrated to pH 8.0 with HCl. dH_2O was added to a total volume of 100 mL.
- 5 mg/mL Lysozyme
- 20,000 U/mg DNAse I
- Sonicator with 3 mm tapered microtip probe, Vibracell
- Sterile filter, 0.22 µm
- Centrifuge, Beckman Coulter Avanti ™ J-25 with JA-10 rotor
- Centrifuge tubes, 250 mL
- Cellstar® tubes, 50 mL

Procedure:

Bacterial culture (600 mL) containing expressed ChiG (from section 3.2.1.) was transferred to 250 mL centrifuge tubes and centrifuged using a JA-10 rotor for 10 minutes at 7168 × *g* and 4 ºC. After decanting off the culture supernatant, the cell pellet was resuspended in 8 ml 20 mM Tris-HCl pH 8.0. Before lysis, 0.001 g lysozyme in 100 µL TrisHCl pH 8.0 and 1 µL DNase I solution (20,000 U/mg) were added per 10 mL cell suspension, followed by incubation for 20 minutes at room temperature. Sonication was performed, using a 3 mm tapered microtip probe, for a time period of 10 minutes running a 5 sec on/off cycle with an amplitude of 27 %. Subsequently, the suspension was centrifuged at 17,418 × *g* and 4 ºC in 10 minutes, before passing the supernatant through a 0.22 µm sterile filter. The resulting cell free extract was stored in a 50 mL Cellstar® tube at 4 ºC until use.

3.2.4 Immobilized-metal affinity chromatography

Immobilized-metal affinity chromatography is a method commonly used when purifying proteins that have been N- or C-terminally fused to a stretch of histidine residues ("His-tag"). Histidine has a strong affinity to certain divalent metal ions (e.g. Ni^{2+} and Co^{2+}), and this is taken advantage of during purification. The metal resin attracts the "his-tagged" proteins, while other proteins do not bind and pass through the column. By applying an eluent containing a high concentration of imidazole (the side-chain moiety of histidine) histidine-tagged proteins are eluted because of competition with imidazole.

Materials:

- BioLogic LP chromatographic system (BioRad)
- Column: Econo-Pac® Chromatography column (1.5 x 12 cm) with Econo-Pac flow adaptor (BioRad)
- Ni-NTA beads (Qiagen)
- Buffer A (binding buffer)
    - 100 mM TrisHCl pH 8.0
    - 20 mM Imidazole
- Buffer B (elution buffer)
    - 100 mM TrisHCl pH 8.0
    - 100 mM Imidazole
- 50 mL Cellstar® tube

Procedure:
To purify ChiG, a resin consisting of nickel-containing agarose beads (3 mL) was chosen. After purging the system and conditioning the Econo-Pac® Chromatography column with buffer A, the protein extract containing ChiG was passed through the column at a flow rate of 1.5 mL/min. Once all unbound protein had passed through the column and the UV-signal had returned to a stable baseline, the running buffer was changed to buffer B (elution buffer). The latter buffer contains a higher concentration of imidazole which releases the His-tagged protein from the column. Fraction containing ChiG were pooled in a 50 mL Cellstar® tube and stored at 4 ºC until further use.

3.2.5 Protein concentration and buffer exchange

Materials:

- Amicon® Ultra 4 10 K centrifugal filter device (Millipore)
- 20 mM Tris-HCl pH 8.0 (see section 3.2.3)
- Eppendorf Centrifuge 5430 R
- Eppendorf tube, 1.5 mL

Procedure:
To concentrate purified protein, the fraction containing ChiG was added to an Amicon® Ultra 4 10 K centrifugal filter device and centrifuged at 4500 × *g* and 4 ºC until the volume of the concentrate was approximately 1 ml. By diluting the concentrated protein in 10 mL 20 mM Tris-HCl pH 8.0 and repeating the centrifugation step, the buffer was exchanged. After five cycles of dilution/concentration, the buffer was considered exchanged and the concentrated protein was stored in a 1.5 mL Eppendorf tube at 4 ºC until further use.

3.3 Quantification of protein concentrations

Protein concentration was measured using the Bradford micro-assay which allows determination of protein concentrations in the range of 1.2-10 µg/mL. The Bradford assay involves binding of a dye, Coomassie Brilliant Blue G-250, to the protein causing a shift in the absorption maximum of the dye from 465 nm to 595 nm (Bradford, 1976). Protein concentration is quantified by measuring the maximum absorbance at the latter wavelength with a spectrophotometer and using a standard curve to convert the measurement from absorbance to µg/mL.

Materials:

- 20 mM TrisHCl pH 8.0 (see section 3.2.3)
- BioRad Protein Assay dye reagent (containing Coomassie Brilliant Blue G-250)
- Protein solution of unknown concentration
- BSA standard curve (1.2-10 µL) provided by Anne Cathrine Bunæs
- Eppendorf Biophotometer
- Disposable 1,5 mL cuvettes (Brand)

Procedure:
Concentrated protein solutions had to be diluted with 20 mM TrisHCl pH 8.0 to fit the measuring range. After dilution, 800 µL protein solution and 200 µL BioRad Protein Assay dye reagent were mixed and incubated for 5 minutes at room temperature before measuring the absorbance at 595 nm. A blank sample was made without the protein, to correct for any other absorbance. The Eppendorf Biophotometer contained a standard curve of BSA ranging from 1.2-10 µL, immediately converting the absorbance to µg/mL. Protein concentrations were calculated by using the mean of three parallels and correction for the dilution factor.

3.4 Polyacrylamide gel electrophoresis of proteins

Polyacrylamide gel electrophoresis performed in denaturing conditions is a method that separates proteins by size. If used with a suitable protein standard, the method can also give an estimation of protein size. In this thesis, the chemicals from the NuPAGE® Elecrophoresis system from Invitrogen™ was used, which is based on a method similar to the traditional sodium dodecyl sulphate polyacrylamide gel electrophoresis method described by Laemmli (1970). The NuPAGE® system uses lithium dodecyl sulphate sample buffer to denature the secondary and non-covalent tertiary structures of the protein, and leave it with a negative charge that is correlated to protein length (i.e. fixed amount of charge per residue). The reducing agent is dithiothreitol, which reduces (breaks) covalent disulphide bonds. Separation of proteins according to size is obtained by protein migration in an electric current through a gel, towards a cathode. Small proteins travel faster than larger proteins because they more easily pass the pores of the polyacrylamide gel. A trihalo compound in the gel covalently binds to tryptophan residues within the protein when exposed to ultraviolet light, causing fluoresce, which can be detected.

Materials:

- BioRad Stain-free gel, 10%, 10 wells
- BioRad 10x Tris/Glycerine/SDS (TGS) Buffer
- NuPAGE® 4x LDS Sample buffer
- NuPAGE® 10x Sample Reducing Agent
- BioRad PowerPac 300 Elecrophoresis Power Supply
- BioRad Electrophoresis Cell, Mini-protean tetra cell
- Bench Mark™ protein ladder, 10-220 kDa (Novex®)
- BioRad Gel Doc™ EZ Imager
- Software: Image lab
- BioRad Stain-Free tray
- Stuart Water bath

Procedure:

A "NuPAGE mixture" was made consisting of 750 µL NuPAGE® 4x LDS Sample buffer, 300 µL NuPAGE® 10x Reducing agent and 450 µL dH_2O. The protein sample was prepared by adding 10 µL NuPAGE mixture to 10 µL sample, followed by boiling for 4 minutes in a Stuart water bath to denature the protein and give it an uniform negative charge. The inner and outer chambers of the electrophoresis cell were filled with 1x TGS-buffer and 10 µL of the samples or 3 µL of bench mark ladder were loaded into the wells in the gel. Electrophoresis was carried out by applying 250 V and 400 A for approximately 20 minutes. Subsequently, the gel was transferred to a stain-free tray and the GelDoc™ EZ Imager instrument from BioRad was used to scan the gel for visualizing the proteins. Further processing of pictures was done using the Image Lab software.

3.5 Enzyme assays

3.5.1 Chitooligosaccharide assays

Using natural substrates to perform chitinase assays is more accurate than using artificial substrates, and the feasibility of determining kinetic parameters of chitinases with natural substrates using high-performance liquid chromatography (HPLC) has been demonstrated by Krokeide et al. (2007). Here, this method is adapted, using Dionex Ultimate 3000 HPLC system with column Rezex RFQ-Fast Acid H+ (8%) and pre-column carbo-H from Phenomenex (see section 3.6.1). Kinetic characterization of ChiG was carried out using the substrates tri-acetyl chitotriose $(GlcNAc)_3$, tetra-acetyl chitotetraose $(GlcNAc)_4$ and penta-acetyl chitopentaose $(GlcNAc)_5$. In addition, ChiG was kinetically characterized at various pH values, ranging from pH 4.0 to pH 8.0 using $(GlcNAc)_4$ as substrate.

Materials:

- Purified ChiG (35.82 µM solution in 20 mM TrisHCl pH 8)
- 1 mg/mL BSA
- 10 mM Tri-acetyl chitotriose
- 10 mM Tetra-acetyl chitotetraose
- 10 mM Penta-acetyl chitopentaose
- 50 mM Sulfuric acid
- 200 mM TrisHCl buffer pH 8.44
    - 2.428 g Trisbase
    - 6 M HCl

      Trisbase was dissolved in 90 mL dH_2O, and titrated to pH 8.44 with HCl. dH_2O was added to a total volume of 100 mL.
- 200 mM BisTris buffer pH 7.32
    - 4.184 g Bis-trise base
    - 6 M HCl

      Bis-tris base was dissolved in 90 mL dH_2O, and titrated to pH 7.32 (room temperature 21ºC) with HCl. dH_2O was added to a total volume of 100 mL.
- 200 mM BisTris buffer pH 6.33
    - 4.184 g Bis-tris base
    - 6 M HCl

Bis-tris base was dissolved in 90 mL dH_2O, and titrated to pH 6.33 (room temperature 20 ºC) with HCl. dH_2O was added to a total volume of 100 mL.

- Sodium acetate buffer pH 5.0
  - 0.1 M Acetic acid
  - 0.1 M Sodium acetate

  After preparing the solutions, 357 mL acetic acid and 643 mL sodium acetate were mixed (recipe taken from: http://delloyd.50megs.com/moreinfo/buffers2.html#acetate)
- Sodium acetate buffer pH 4.0
  - 0.1 M Acetic acid
  - 0.1 M Sodium acetate

  After preparing the solutions, 847 mL acetic acid and 153 mL sodium acetate were mixed (recipe taken from: http://delloyd.50megs.com/moreinfo/buffers2.html#acetate)
- Eppendorf ThermoMixer C

NB. Buffers at pH 8.44, 7.32 and 6.33 are exactly 8.0, 7.0 and 6.0 at 37 ºC, which is the temperature at which the enzyme assays are performed. Recipes are taken from: http://www.bioinformatics.org/jambw/5/4/index.html.

Procedure:

Reaction mixtures were prepared by mixing chitin oligosaccharides, buffer and BSA according to Tables 3.1, 3.2 and 3.3. Assays at different pH was prepared according to Table 3.2 except with use of the additional buffer stock solutions listed above. Reactions were started by adding ChiG to the prepared samples placed in an Eppendorf ThermoMixer C operating at 37 ºC and 300 rpm. ChiG was added to each reaction mixture with 20 seconds intervals. 10, 20 and 30 minutes after starting the reaction start, 50 µL of the reaction mixture was taken out and mixed with a stop solution, containing 50 µL 50 mM sulphuric acid, in a HPLC vial. All samples were analysed by HPLC the same day as the assay was performed (see section 3.6.1). The initial activity testing is described in section 3.5.2.

Table 3.1. Setup of reactions with $(GlcNAc)_3$. Samples with different substrate concentrations were prepared as indicated and dH_2O was added to a final volume of 250 µL. Reactions were started by adding the enzyme solution. The stock solutions were: 10 mM tri-acetyl chitotriose, 200 mM bis-tris pH 6.33, 1 mg/mL BSA and 100 nM ChiG.

Substrate concentration, µM	Tri-acetyl chitotriose, µL	Bis-tris pH 6, µL	BSA, µL	ChiG, µL
300	7.5	25	25	25
600	15	25	25	25
900	22.5	25	25	25
1800	45	25	25	25
3600	90	25	25	25
5400	135	25	25	25
Final concentration	See first column	20 mM	0.1 mg/mL	10 nM

Table 3.2. Setup of reactions with $(GlcNAc)_4$. Samples with different substrate concentrations were prepared as indicated and dH_2O was added to a final volume of 250 µL. Reactions were started by adding the enzyme solution. The stock solutions were; 10 mM tetra-acetyl chitotetraose, 200 mM bis-tris pH 6.33, 1 mg/mL BSA and 10 nM ChiG.

Substrate concentration, µM	Tetra-acetyl chitotetraose, µL	Bis-tris pH 6, µL	BSA, µL	ChiG, µL
100	2.5	25	25	25
200	5	25	25	25
400	10	25	25	25
600	15	25	25	25
1000	25	25	25	25
1400	35	25	25	25
2000	50	25	25	25
3000	75	25	25	25
Final concentration	See first column	20 mM	0.1 mg/mL	1 nM

Table 3.3. Setup of reactions with $(GlcNAc)_5$. Samples with different substrate concentrations were prepared as indicated and dH_2O was added to a final volume of 250 µL. Reactions were started by adding the enzyme solution. The stock solutions were; 10 mM penta-acetyl chitopentaose, 200 mM bis-tris pH 6.33, 1 mg/mL BSA and 10 nM ChiG.

Substrate concentration, µM	Penta-acetyl chitopentaose, µL	Bis-tris pH 6, µL	BSA, µL	ChiG, µL
100	2.5	25	25	12.5
200	5	25	25	12.5
400	10	25	25	12.5
600	15	25	25	12.5
800	20	25	25	12.5
1200	30	25	25	12.5
2000	50	25	25	12.5
Final concentration	See first column	20 mM	0.1 mg/mL	0.5 nM

3.5.2 Initial activity testing

To select the intervals of substrate concentrations for the chitooligosaccharides, initial testing of the activity was required. $(GlcNAc)_4$ was the starting point for the analysis, and a concentration of 200 µM was initially used with varying concentration of ChiG (10 nM, 50 nM and 100 nM). Further, an interval of concentrations (100-1200 µM) was chosen for $(GlcNAc)_{4,}$, and analysis of the kinetic data indicated whether to increase or decrease the substrate concentrations. Optimally, the substrate concentrations should be 0.2-5 × K_m. Determination of enzyme and substrate concentration for $(GlcNAc)_3$ and $(GlcNAc)_5$ was done based on activity on $(GlcNAc)_4$.

3.5.3 Degradation of polysaccharides

Materials:

- Arabinoxylan from wheat
- Cellulose
- Pectin
- Xylan from aspen
- Xanthan gum
- Betaglucan from barley
- Galactomannan from Guar
- Galactomannan from Konjak
- Alginate
- Galactomannan from Locus bean gum
- Lichenan
- Eppendorf Centrifuge 5418R
- Biosan Rotator-mixer, Multi RS-60
- 35.82 µM ChiG (in 20 mM TrisHCl pH 8)

Procedure:

After mixing each substrate in dH_2O to a final concentration of 5 mg/mL, the polysaccharide solutions were put on a Biosan rotator-mixer at 35 rpm, 60º angle and 50 ºC over night to dissolve. 1 mL solution was centrifuged for 5 minutes at 16,900 x *g* and 100µL portions of the supernatants were transferred to HPLC vials. ChiG (1 µl of a 35.83 µM solution in 20 mM TrisHCl pH 8) was added to one parallel of the substrates and another parallel was used as a negative control without the enzyme. After incubation at room temperature overnight, the samples were analysed by size-exclusion HPLC, as described in section 3.6.2.

3.5.4 Peptidoglycan degradation assay

Materials:

- 50 µg/µl peptidoglycan from *Streptococcus pneumoniae* (In-house made by Daniel Straume)
- Bacterial cell wall fragments (see section 3.5.1)
- 35.82 µM ChiG (in 20 mM TrisHCl pH 8)
- 5 mg/mL mutanolysin (in dH_2O)
- 10 µM lysozyme (in 20 mM TrisHCl pH 8.0)
- 200 mM Bis-tris pH 6.33
- Water bath (Julabo)

Procedure:

A time course assay with purified peptidoglycan and cell wall fragments as substrates was done in a Julabo water bath at 37 ºC, with sampling after 1 hour, 4 hours and 24 hours. In addition to reactions with ChiG, reactions with mutanolysin and lysozyme were included as positive controls for all the substrates, as well as a negative control that contained additional buffer instead of enzyme. In each individual reaction, peptidoglycan was added to a concentration of 5 µg/mL, whereas for reactions with cell wall fragments 1.5 µL cell wall fragments of unknown concentration were added to a total reaction mixture of 15 µL. Other components in the reaction mixtures were Bis-Tris pH 6.33 at a final concentration of 20 mM and 1 µM of enzyme. Activity was measured qualitatively by MALDI-TOF MS according to section 3.8.

3.5.5 Preparation of bacterial cell walls

Preparation of cell wall fragments from various Gram positive bacteria was performed in order to assay for novel ChiG activities. The crude cell wall preparation method was based on a protocol by Räsänen and Arvilommi (1981).

Materials:

- Selected bacterial strains
- Brain-Heart-Infusion (BHI) medium (section 3.1.1)
- De Man, Rogosa, Sharpie (MRS) medium (section 3.1.1)
- GM17 medium (section 3.1.1)
- 5 mg/mL RNase B
- 20,000 U/mg DNase I
- 200 µg/mL Trypsin (solved in 0.01% acetic acid)
- Phosphate-buffered saline
    - 0.8 g NaCl
    - 0.02 g KCl
    - 0.144 g Na_2HPO_4
    - 0.024 g KH_2PO_4

      The reagents was dissolved in 80 mL dH_2O and pH was adjusted to 7.4 using HCl. After adding dH_2O to a final volume of 100 mL, the buffer was autoclaved at 121 ºC in 15 minutes.
- Glass beads, acid washed (Sigma-Aldrich)
- MP Biomedicals FastPrep®-24
- Eppendorf Centrifuge 5430 R
- Eppendorf Centrifuge 5418 R
- Water bath

Procedure:

Three different bacteria were chosen for the cell wall samples: *L. plantarum*, *E.faecalis*, and *L. lactis*. The bacteria were cultivated according to section 3.1.1. Bacterial cultures were centrifuged at 7168 × *g* and 4 ºC using Eppendorf Centrifuge 5430 R, and cell pellets were washed two times with dH_2O. Cells were then lysed subsequent to resuspending the cell pellet (approximately 200 µL) in 1 mL PBS, and addition of 0.5 g of acid washed glass beads.

Using MP Biomedical FastPrep®-24, which was applied at speed of 5 M/S for 20 seconds (three times), causing vigorous shacking of the cell-containing samples, lysed the cells. The resulting suspension was centrifuged twice at 1500 rpm for 15 minutes using Eppendorf Centrifuge 5418 R (used through the rest of the procedure), and the supernatant containing cell wall fragments was collected. Sedimentation of fragments was done by centrifugation at 15,000 rpm for 30 minutes, and the pellet was subsequently washed three times with phosphate-buffered saline. To destroy RNA and DNA, 100 µg RNase B and 50 µg DNase I were added, and the suspension was incubated approximately one hour at room temperature. Subsequently trypsin was then added to the sample to a final concentration of 20 µg/mL, followed by incubation at 37 ºC and 300 rpm for 2.5 hours in order remove protein. Lastly, the solution was washed three times with PBS and boiled to inactivate trypsin.

3.6 High Performance Liquid Chromatography

High Performance Liquid Chromatography (HPLC) is a method for separation of biomolecules that gives higher resolution, sensitivity, and accuracy as well as shorter analysis times, compared to classic liquid chromatography. A mobile phase is passed through a column material (stationary phase) by a high-pressure pump. Sample is injected before the column, using a specialized injector device, and a detector monitors the eluents (Figure 3.1). The principle of separation depends on the choice of column, but common for them all is that separation is obtained by analyte interactions with both the mobile and stationary phase.

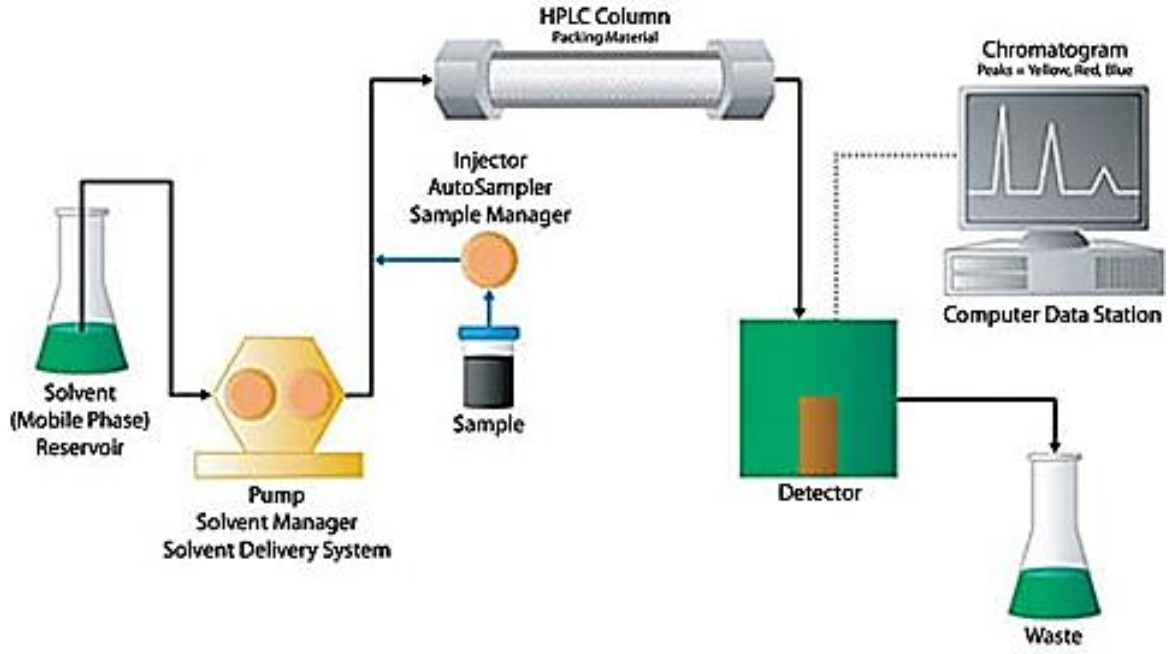

Figure 3.1. High-Performance Liquid chromatography system. The liquid mobile phase is passed through the HPLC column, containing the stationary phase, by a high-pressure pump. Sample is injected, separated in the column and detected, before ending up in waste along with the mobile phase. When used in a preparative mode, selected fractions are collected.

3.6.1 Ion exclusion chromatography

Ion exclusion chromatography is a method commonly used to separate weak organic acids. The resin consists of a cation exchange polymer, and molecules are separated by size caused by the Donnan principle between the stationary phase and the mobile phase. In this thesis, the method was used to separate chitooligosaccharides of different lengths, and subsequently quantify the amounts of products generated after doing chitooligosaccharide activity assays (described in section 3.5).

Materials:

- Dionex Ultimate 3000 HPLC system
- Column: Rezex RFQ-Fast Acid H+ (8%). Particle size: 8 µm.
  Dimensions: 7.8 x 100 mm (Phenomenex)
- Pre-column: Security guard cartridge carbo-H. Dimensions: 4 x 3 mm (Phenomenex).
- Software: Dionex™ Chromeleon™ 7.2 CDS
- Eluent: 5 mM sulphuric acid

Procedure:
Quantification of chitooligosaccharides was done using a Dionex Ultimate 3000 UHPLC instrument, with Rezex RFQ-Fast Acid H+ (8%) column and a security guard cartridge carbo-H 4x3 mm. The HPLC was made ready for operation by applying a flow of 0.3 mL/min (of 5 mM sulphuric acid) on the column, setting the column oven temperature to 85 ºC and initiating the UV-lamp. The flow was changed to 1 mL/min before injecting samples (5 µL) on the column. The run-time was 6 minutes, and analytes were detected using absorption of ultraviolet light at 194 nm.

3.6.2 Size exclusion chromatography

Size exclusion chromatography (SEC) is a technique that separates macromolecules based on their hydrodynamic volume. Macromolecules with small enough hydrodynamic volumes can enter the pores, leading to increased retention time depending on their size/shape. Larger molecules do not easily enter the pores (if they enter at all) and travel faster through the column. The separation achieved depends on the pore size of the chromatographic resin (stationary phase). In this study, the SEC method was used to study hydrolysis of soluble polysaccharides by an enzyme. If a polysaccharide is cleaved by an enzyme, the molecular size of the polysaccharide will be reduced, leading to an average increase in retention time (observed as a shift the polysaccharide peak in the chromatogram).

Materials:

- Polysaccharides (see section 3.5.5)
- Dionex Ultimate 3000 UHPLC systems
- Columns:
    1. TSK-GEL G3000PW_{XL}. Particle size: 6 µm. Dimensions: 7.8 x 300 mm (Sigmaaldrich)
    2. TSK-GEL G-OLIGO-PW. Particle size: 6 µm. Dimensions: 7.8 x 300 mm (Sigmaaldrich)
- Pre-column: BEH Amide VanGuard. Particle size: 1.7 µm. Dimensions: 2.1 x 5 mm (Waters corp., USA)
- Eluent: 0.1 M $NaNO_3$

Procedure:
Qualitative analysis of ChiG activity on polysaccharides was performed using a UHPLC Dionex Ultimate 3000 instrument with pre-column BEH Amide VanGuard (2.1 mm x 5 mm), column TSK-GEL G3000PW$_{XL}$ (7.8 x 300 mm) and column TSK-GEL G-OLIGO-PW (7.8 x 300 mm) connected in series. Separation was obtained by applying a column temperature at 85 ºC and flow at 1 mL/min with 0.1 M $NaNO_3$ as eluent. 20 µL sample was injected on the column with a run time of 30 minute and refractive index detection.

3.7 Analysis of kinetic data

The velocities for each substrate concentration were calculated by measuring absorbance (peak area) of product formation as a function of time (minutes). The slope of the linear correlation is the velocity. Using a standard curve (see appendix Figure A1), peak areas were converted to product concentrations. Michaelis-Menten plots were generated using direct fitting to the Michaelis-Menten equation using GraphPad Prism (substrate as a function of velocity). Values for K_m and k_{cat} were obtained from the plots, according to theory presented in section 1.5.

3.8 Matrix-assisted laser desorption/ionisation time-of-flight MS

In mass spectrometry (MS), the general principle is to separate ionized, and occasionally fragmented, analytes according to their mass-to-charge ratios (*m/z*) (Miller, 2005). This requires an ion source, a mass analyser and a detector connected to a computer. Matrix-assisted laser desorption/ionisation time-of-flight (MALDI-TOF) MS is a mass spectrometry method which is used to analyse biopolymers and large organic molecules. The ionization method is MALDI, and in this step, laser irradiation causes desorption and ionization of analytes embedded in a solid matrix on a target plate. TOF refers to the analyser type, and as the name indicates, mass separation is obtained by capitalizing on the differences in the time it takes each ion to travel a certain distance in an electric field. Larges ions travel more slowly than smaller ones. A signal is detected when an ion hits the detector, after reflection (Figure 3.2). A mass spectrum is generated by plotting *m/z* as a function of the ion current.

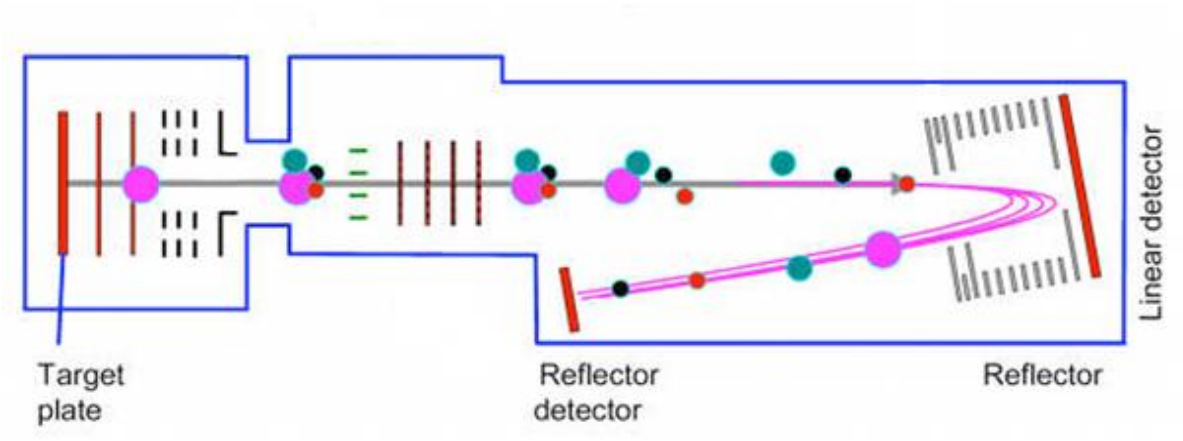

Figure 3.2. A schematic illustration of MALDI-TOF MS. Molecules embedded in a solid matrix are desorbed and ionized with a laser. The ions travel through an electric field and are separated based on their time-of-flight. The reflector creates a longer distance for the ions to travel, before they are detected. The picture was taken from: http://www.giga.ulg.ac.be/jcms/cdu_15169/maldi-tof/tof-bruker-ultraflex-ii-tof/tof-april-2005.

Materials:

- 2,5-dihydroxybenzoic acid (DHB)
  - 4.5 mg DHB
  - 140 µL acetonitrile
  - 350 µL dH_2O
- Bruker Daltonics Ultraflex TOF/TOF
- MTP 384 Target plate ground steel TF
- MTP Target frame III
- Selected samples
- Software: FlexControll and FlexAnalyzer

Procedure:

After spotting 2 µL DHB matrix onto a MTP 384 Target plate, 1 µL of selected sample was immediately mixed with the matrix and dried. Analysis of the samples was performed using the mass spectrometer Ultraflex TOF/TOF from Bruker Daltonics with the software FlexControl. The target plate was injected in the instrument placed in a MTP Target frame III. In FlexControl, the positions of analytes embedded in the solid DHB matrix was chosen, and intensity of laser irradiation was controlled. Samples were irradiated with 15-30 % of maximum laser intensity. In FlexAnalyzer the obtained mass spectra was inspected.

3.9 Antifungal assay

Materials:

- Potato Dextrose Agar (PDA)
    - 24 g Difco™ potato dextrose broth
    - Agar agar

      The potato dextrose broth was added dH_2O to a final volume of 1 litre, and autoclaved at 121 ºC in 15 minutes. 1.5 % agar was added before transferring to petri dishes.
- Fungus: *Trichoderma reesei*, QM6a
- ChiG (35.83 µM in 20 mM TrisHCl pH 8)
- 20 mM TrisHCl pH 8.0
- Mixture of extracellular proteins from *Serratia marcesens* grown on chitin (in 10 mM Bis-Tris pH 6.2; kindly provided by Sophanit Mekasha)
- 10 mM Bis-Tris pH 6.33

Procedure:

A fungal conidia spore suspension was prepared by scraping spores from a -80 stock solution with a sterile toothpick and mixing with 100 µL dH_2O. The resulting suspension was spread on PDA plates and incubated at 30 ºC. After observing hyphal extension, a piece of agar containing hyphae was extracted and placed in the middle of a new PDA plate. Wells for enzyme solutions were made 1-2 mm from new hyphal extensions after incubation overnight. 20 µL enzyme solution at different concentrations was pipetted into the wells. One well did not contain enzyme, solely buffer.

4 RESULTS

4.1 Expression and purification of ChiG

His-tagged ChiG was produced recombinantly *in E. coli* and was extracted by periplasmic extraction or cell lysis. Protein gel electrophoresis performed using the NuPAGE® Elecrophoresis system showed that ChiG was well expressed, but present in greater amounts in the cell lysate (cell-free protein extract) compared to the periplasmic extract (Fig 4.1). Figure 4.1 also shows that a considerable amount of ChiG was present in the pellets generated during extract preparation, indicating that a fraction of the produced ChiG was insoluble.

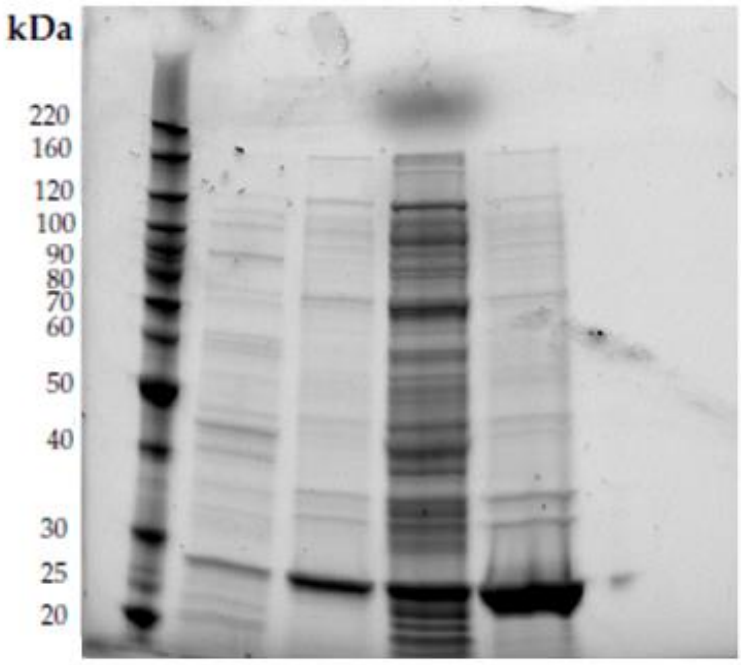

Figure 4.1. Pellet and supernatant for periplasmic extract and lysed cells. Gel lanes: 1, bench mark protein ladder, with masses indicated in kDa; 2, periplasmic extract; 3, pellet generated when preparing the periplasmic extract; 4, cell-free protein extract; 5, pellet generated when preparing the cell-free protein extract. Sample sizes were 3 µL for the bench mark ladder, 10 µL for the extracts (of approximately 45 mL of the original extracts from 600 mL culture) and 10 µL for the pellets (where a piece of the pellets were dissolved in dH_2O).

ChiG was purified from both periplasmic extract and cell lysate using a Ni-column, and the BioLogic LP chromatographic system (low pressure). Even though the chosen resin has a high binding capacity (5 mg protein per mL column material), half of each sample was purified at a time to avoid loss of ChiG. The chromatograms of the purification process also show better yield of ChiG from the cell lysate than from the periplasmic extract (Figure 4.2).

A)

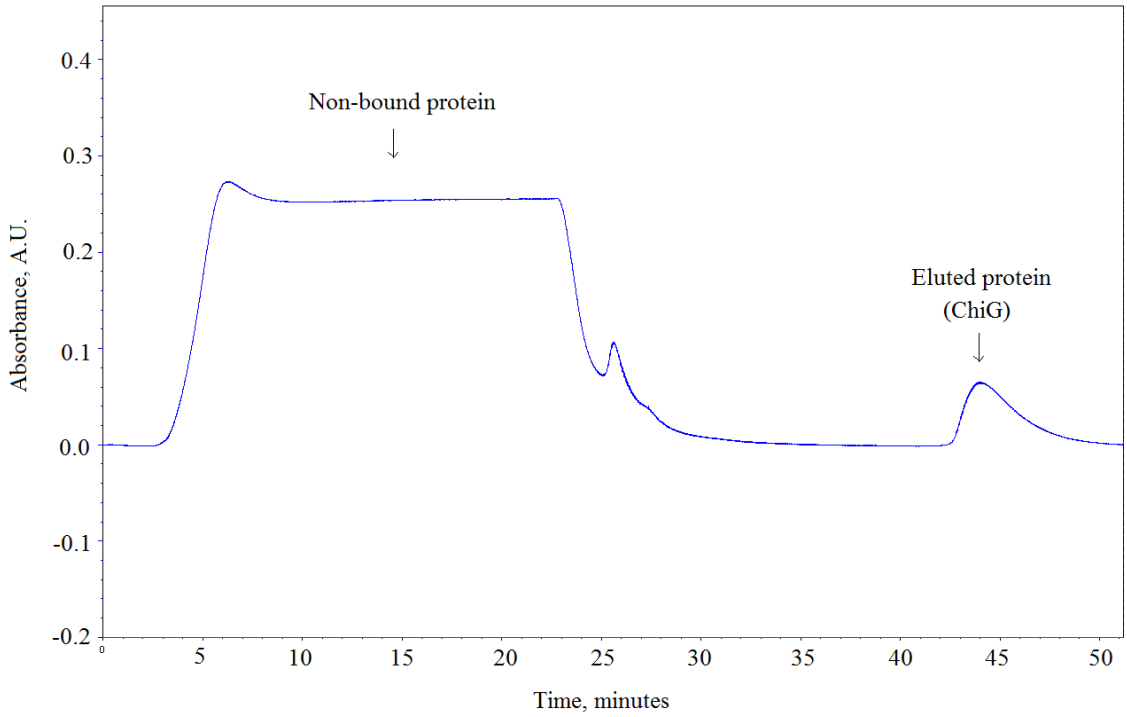

B)

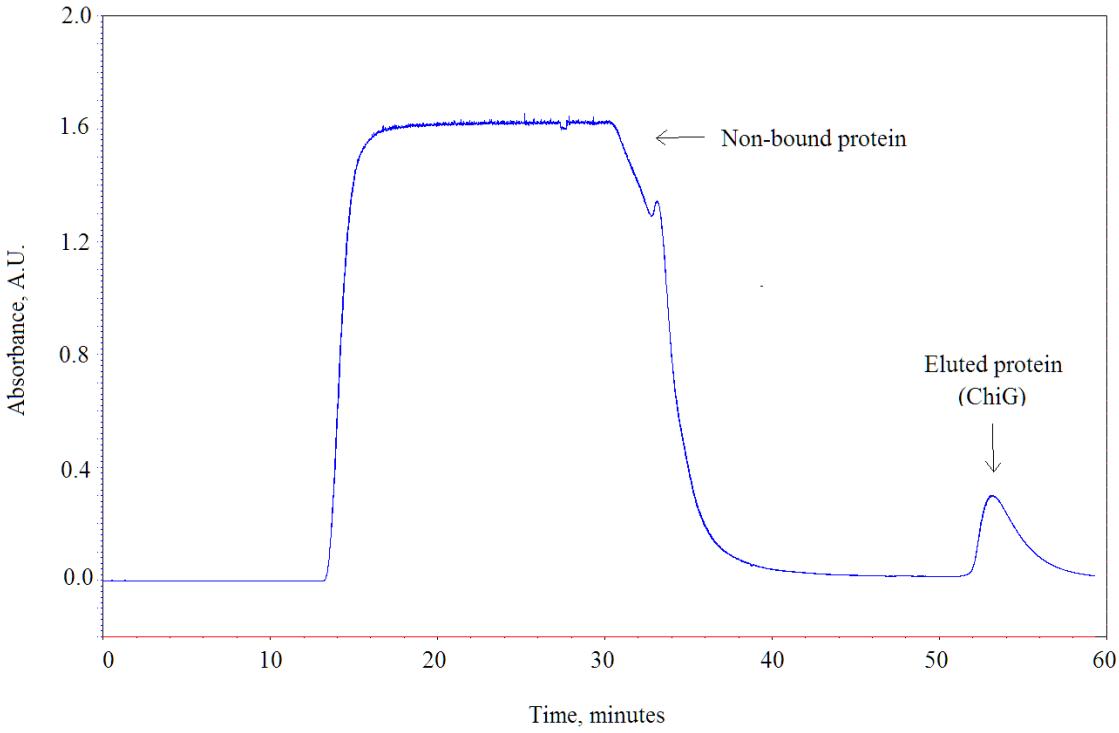

Figure 4.2. Chromatograms of ChiG purification. The pictures show the UV-trace (280 nm) obtained during IMAC purification of ChiG from a periplasmic extract (A) or a cell lysate (B). Peaks representing flow through (non-bound) proteins and eluted ChiG are labelled and indicated by arrows. Sample sizes for the periplasmic extract and the cell lysate were both 45 mL, corresponding to approximately 600 mL of the original culture volumes.

The cell lysate was used in further work and Figure 4.3 shows that ChiG could be purified from this sample, after one round of purification. The final yield of pure ChiG obtained from cell lysates was approximately 1.5 mg per L culture.

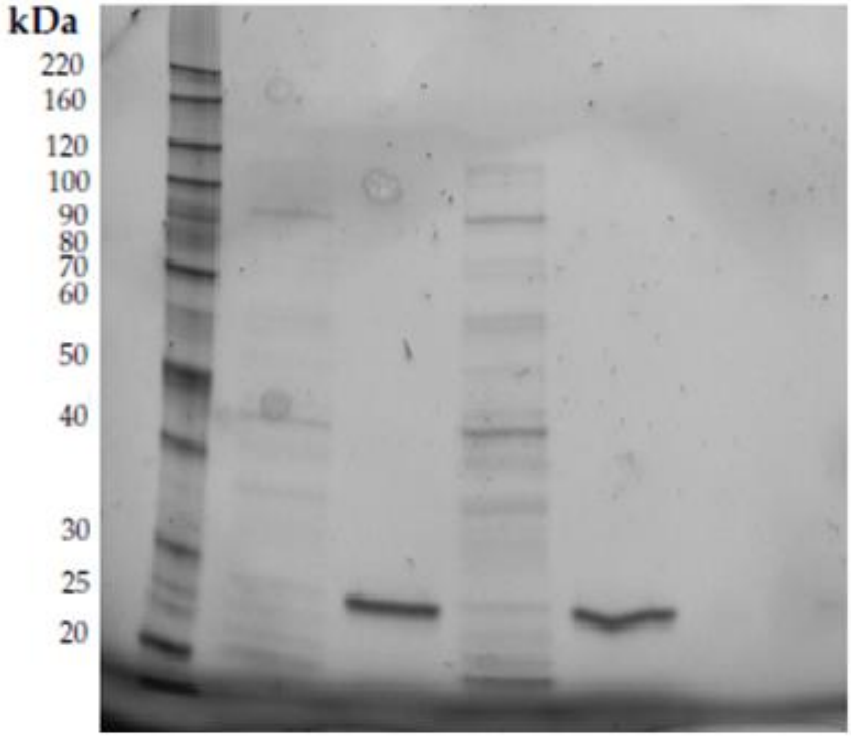

Figure 4.3. Purification of ChiG from cell lysates. Gel lanes: 1, bench mark ladder; 2, non-bound protein; 3, purified ChiG; 4, non-bound protein; 5, purified ChiG. Sample sizes were 3 µL for the bench mark ladder and 10 µL for the other samples. The molecular weight of ChiG is 26 kDa.

ChiG was concentrated in an Amicon® Ultra 4 10 K centrifugal filter device during centrifugation, and the elution buffer (used during purification) was changed to 20 mM TrisHCl pH 8. The final protein concentration was quantified using the Bradford micro-assay method, yielding a concentration of 35.82 µM. Purified and concentrated ChiG was stored in an Eppendorf tube at 4 ºC.

4.2 Kinetic analysis

Kinetic parameters for hydrolysis of $(GlcNAc)_{3-5}$ were determined using quantification of reaction products by HPLC. The influence of pH on the kinetic parameters was also determined for $(GlcNAc)_4$. Table 4.1 summarize the kinetic parameters obtained from the enzyme assays towards chitooligosaccharides of different lengths.

Table 4.1. Kinetic parameters obtained from enzyme assays towards chitooligosaccharides.

Substrate	K_m, **µM**	k_{cat}, s^{-1}	k_{cat} / K_m, $\mu M^{-1}s^{-1}$
$(GlcNAc)_3$	4.9 (± 0.84) × 10^3	215 (± 21)	0.0437
$(GlcNAc)_4$	5.6 (± 0.40) × 10^2	584 (± 14)	1.05
$(GlcNAc)_5$	5.3 (± 0.84) × 10^2	451 (± 28)	0.854

Initially activity testing was done by testing out an interval of substrate concentrations (described in secton 3.5.2), make plots of substrate concentration versus velocity, and analyse the curves. When observing a curve that did not particularly flat out at higher concentrations, the substrate concentrations were increased. When an approximately hyperbolic curve was observed, the enzyme assays were performed in triplicates and the kinetic parameters could be determined.

4.2.1 Activity on $(GlcNAc)_3$

Kinetic parameters for hydrolysis of $(GlcNAc)_3$ were obtained using substrate concentrations ranging from 300-5400 µM and an enzyme concentration of 10 nM. ChiG hydrolysed $(GlcNAc)_3$ to GlcNAc and $(GlcNAc)_2$ (Figure 4.4). Quantification of $(GlcNAc)_2$ formation was used for the determination of K_m and k_{cat}. All velocity curves were linear with R-squared values > 99 % (see Fig 4.5 for an example and see the appendix, Table A1, for an overview of all the R-squared values). Velocities determined for each substrate concentration were fitted to the Michaelis-Menten equation by non-linear regression using GraphPad Prism (Fig 4.6). The K_m and k_{cat} values were determined to be 4.9 (± 0.84) ×10^3 µM and 215 (± 21) s^{-1}, respectively.

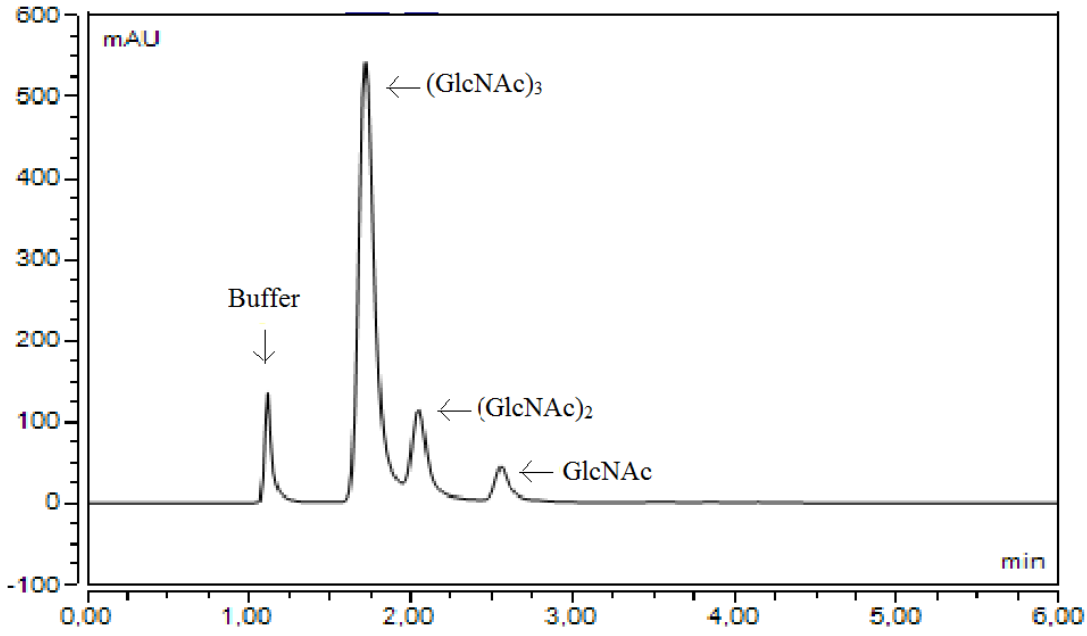

Figure 4.4. Chromatogram of $(GlcNAc)_3$ degradation. The oligosaccharide peaks are indicated by arrows and labeled.

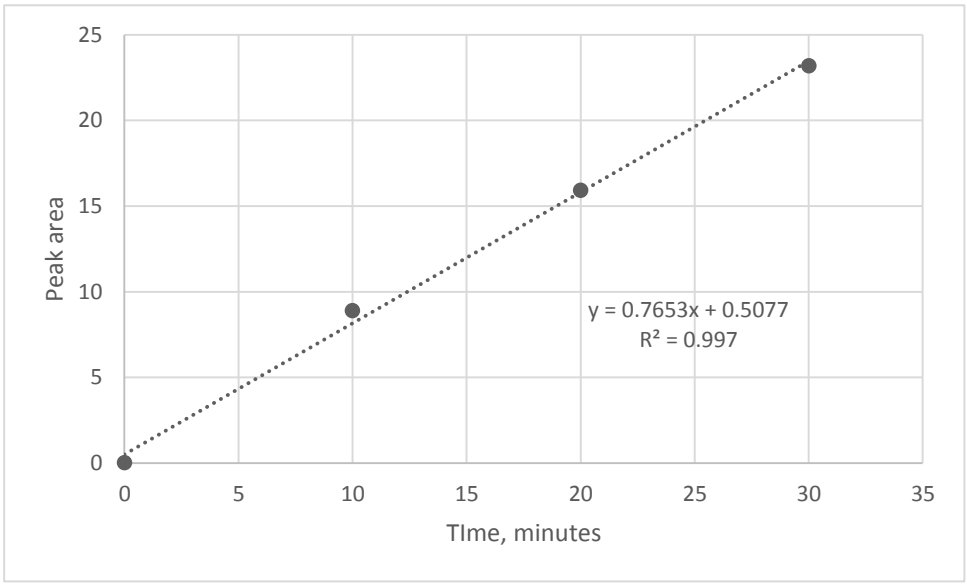

Figure 4.5 Example of formation of $(GlcNAc)_2$ over time during degradation of $(GlcNAc)_3$. Time is plotted as a function of the peak area. The straight line and numbers obtained from linear regression are shown. The substrate concentration was 5400 µM.

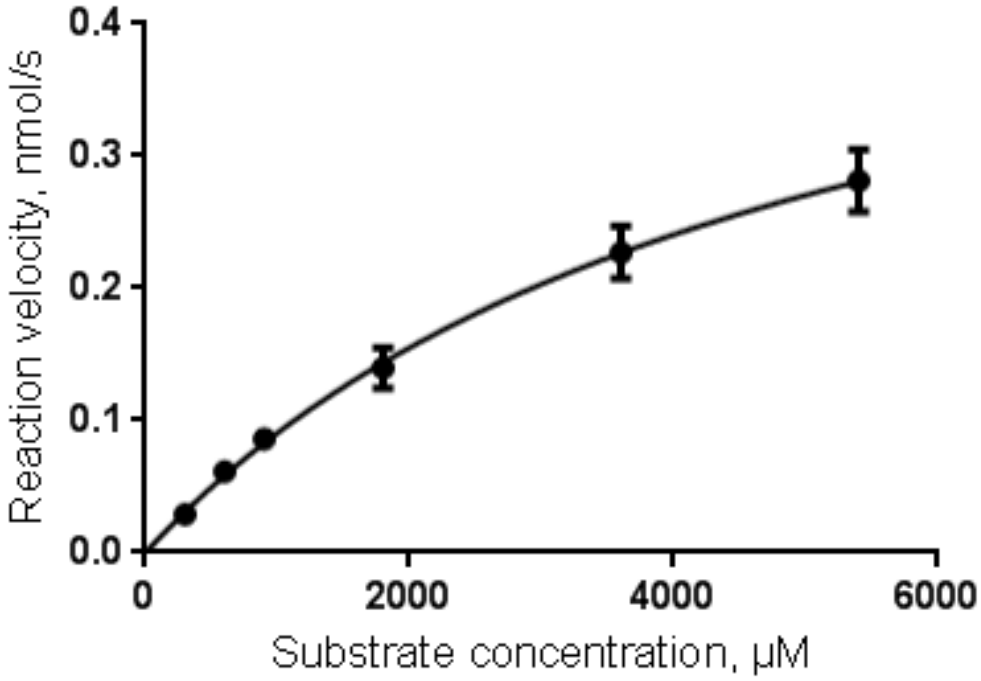

Figure 4.6. Michaelis-Menten plot for ChiG activity towards $(GlcNAc)_3$. The graph shows the datapoints (in this case for only two parallels), with standard deviation, and the curve resulting from direct fitting to the Michaelis Menten equation. Only

4.2.2 Activity on $(GlcNAc)_4$

Kinetic parameters for hydrolysis of $(GlcNAc)_4$ were obtained using substrate concentrations ranging from 100-3000 µM and an enzyme concentration of 1 nM. ChiG hydrolysed $(GlcNAc)_4$ exclusively to $(GlcNAc)_2$ (Figure 4.7). Quantification of $(GlcNAc)_2$ was used for determination of K_m and k_{cat}. All velocity curves were linear with R-squared values > 89 % (see Fig 4.8 for an example and the appendix, Table A1, for an overview of all the R-squared values). Velocities determined for each substrate concentration were analyzed using the Michaelis-Menten equation by non-linear regression using GraphPad Prism (Fig 4.9). The K_m and k_{cat} values were determined to be 556 (± 40) µM and 584 (± 14) s^{-1}, respectively.

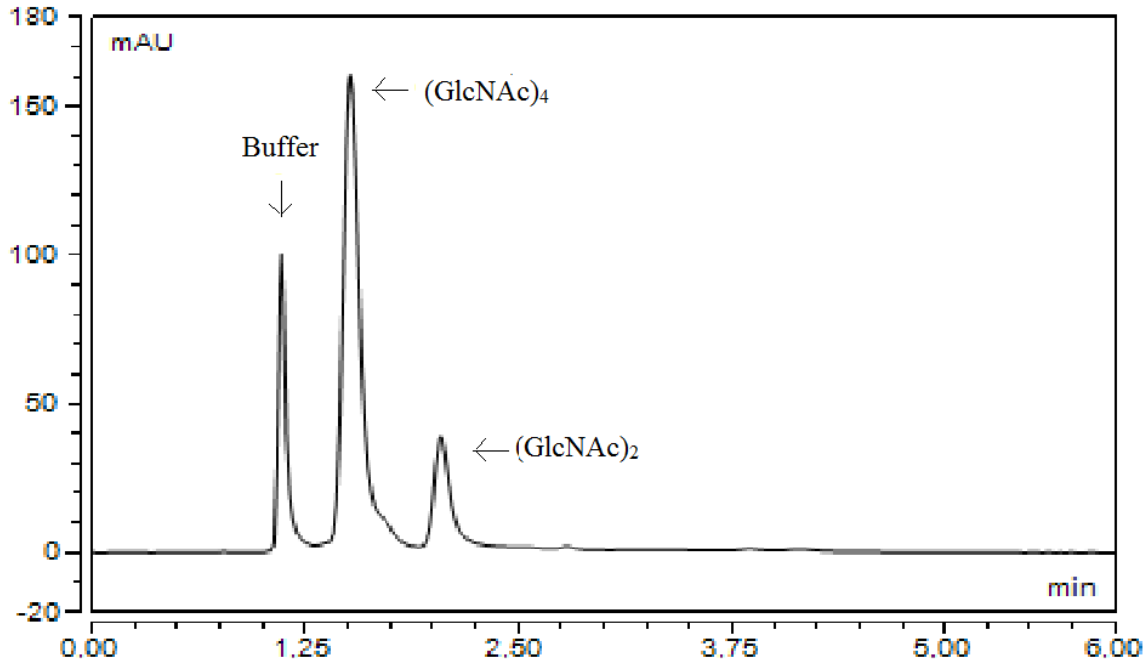

Figure 4.7. Chromatogram of $(GlcNAc)_3$ degradation. The oligosaccharide peaks are indicated by arrows and labeled.

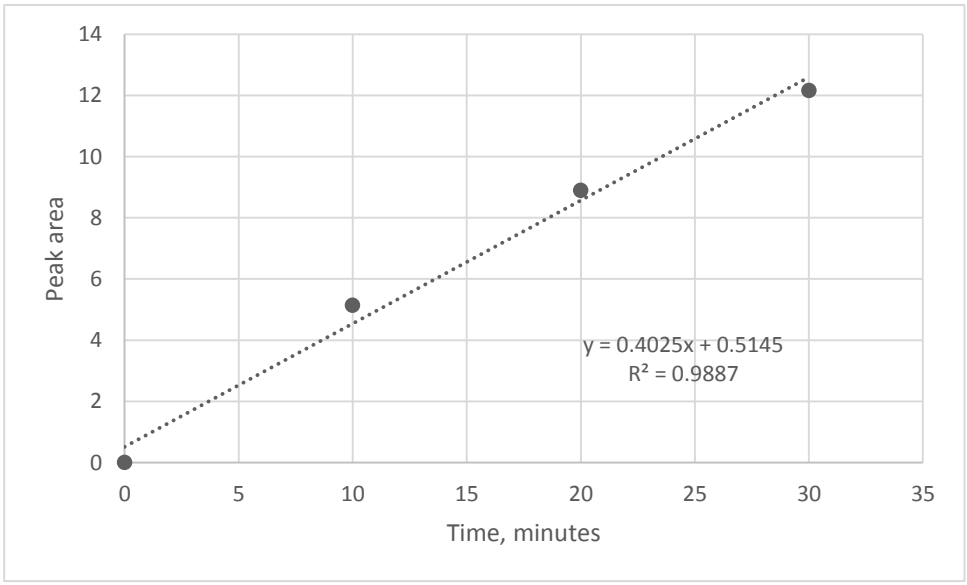

Figure 4.7. Formation of $(GlcNAc)_2$ over time by degradation of $(GlcNAc)_4$. Time is plotted as a function of the absorbance. The linear curve is exemplified by degradation of 600 µM substrate.

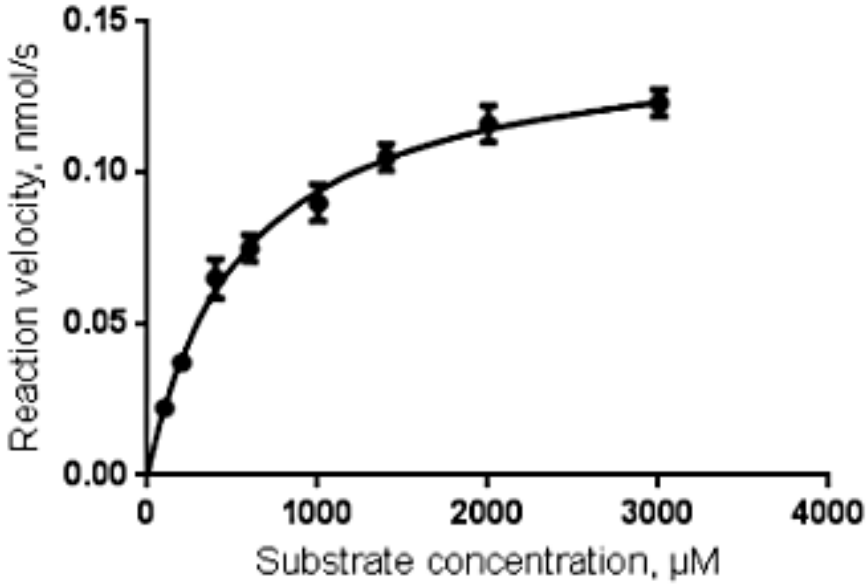

Figure 4.8. Michaelis-Menten plot for ChiG activity towards $(GlcNAc)_4$. The graph shows the datapoints, with standard deviation, and the curve resulting from direct fitting to the Michaelis Menten equation.

4.2.3 Activity on $(GlcNAc)_5$

Kinetic parameters for hydrolysis of $(GlcNAc)_5$ were obtained using substrate concentrations ranging from 100-2000 µM and an enzyme concentration of 0.5 nM. Within the time frame of the assay, ChiG hydrolysed $(GlcNAc)_5$ to $(GlcNAc)_3$ and $(GlcNAc)_2$ only (Figure 4.9). Quantification of $(GlcNAc)_2$ formation was used for the determination of K_m and k_{cat}. All velocity curves were linear with R-squared > 82 % (see Fig 4.10 for an example and see the appendix, Table A1 for an overview of all the R-squared values). Velocities determined for each substrate concentration were analyzed using the Michaelis-Menten equation by non-linear regression using GraphPad Prism (Fig 4.11). The K_m and k_{cat} values were determined to be 528 (± 84) µM and 451 (± 28) s^{-1}, respectively.

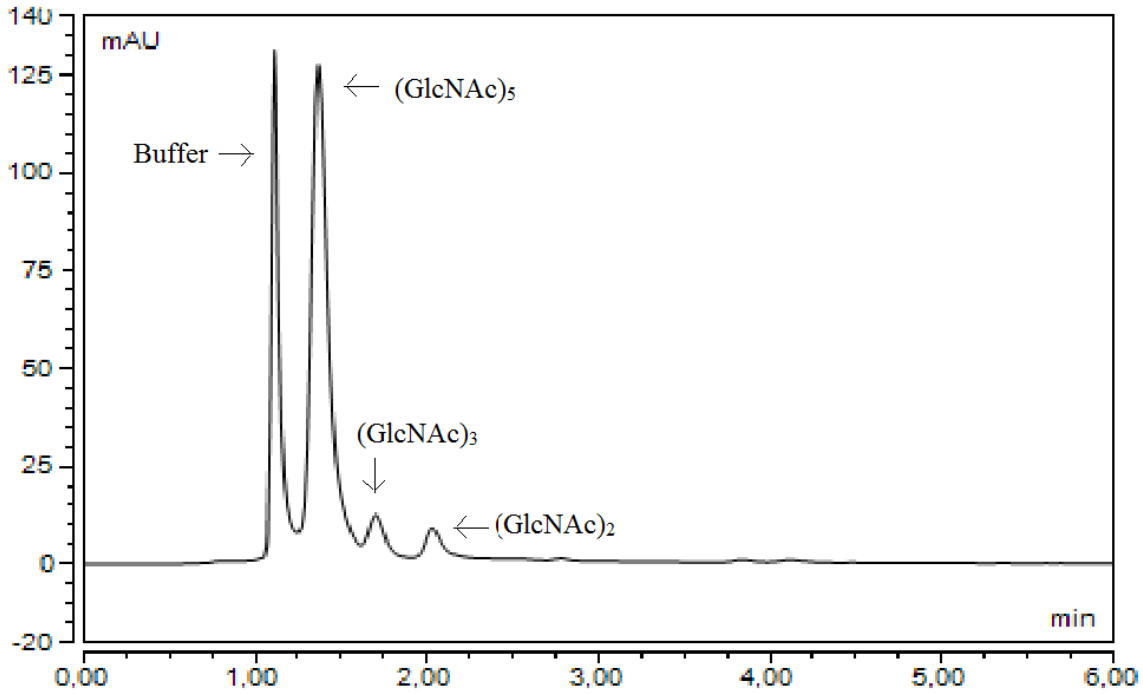

Figure 4.9. Chromatogram for $(GlcNAc)_5$ degradation. The oligosaccharide peaks are indicated by arrows and labelled.

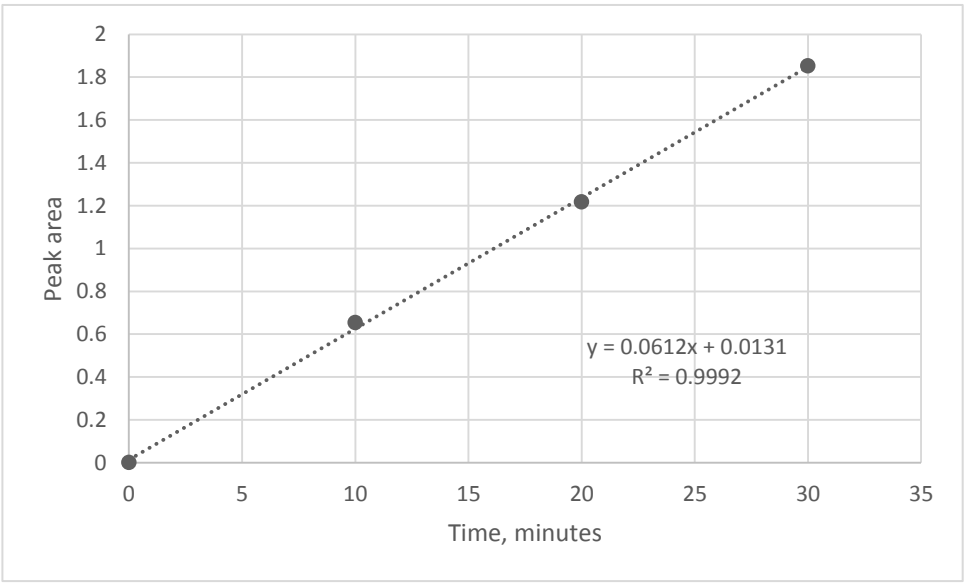

Figure 4.10 Formation of $(GlcNAc)_2$ over time by degradation of $(GlcNAc)_5$. Time is plotted as a function of the absorbance. The linear curve is exemplified by degradation of 200 µM substrate.

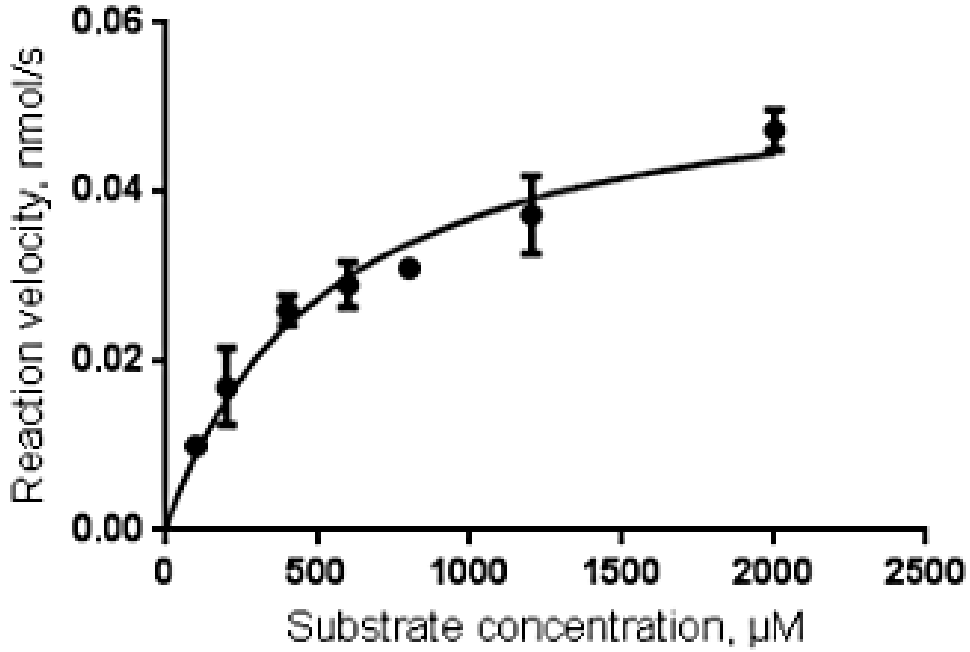

Figure 4.11. Michaelis-Menten plot for ChiG activity towards $(GlcNAc)_5$. The graph shows the datapoints, with standard deviation, and the curve resulting from direct fitting to the Michaelis Menten equation.

4.2.4 ChiG activity at varying pH

Kinetic parameters for ChiG activity at pH 4.0, 5.0, 7.0 and 8.0 were obtained by following the same procedure as for the determination of activity towards $(GlcNAc)_4$ at pH 6.0. All velocities determined were linear with R-squared > 87 % (see the appendix, Table A1, for an overview of all the R-squared values). Velocities determined for each substrate concentration were fitted to the Michaelis-Menten equation by non-linear regression using GraphPad Prism (in the appendix, Figures A2-A5). The kinetic parameters thus obtained are listed in Table 4.1 and the resulting pH profile for k_{cat}/K_m is shown in Figure 4.12.

Table 4.2. Kinetic parameters at pH 4.0, 5.0, 6.0, 7.0 and 8.0.

Substrate	pH	K_m, µM	k_{cat}, s^{-1}	k_{cat} / K_m, $\mu M^{-1}s^{-1}$
(GlcNAc)4	4	7.54 (± 0.97) × 10^2	736 (± 36)	0.976
(GlcNAc)4	5	3.58 (± 0.31) × 10^2	312 (± 7.6)	0.872
(GlcNAc)4	6	5.56 (± 0.40) × 10^2	584 (± 14)	1.05
(GlcNAc)4	7	8.32 (± 1.00) × 10^2	326 (± 18)	0.392
(GlcNAc)4	8	7.67 (± 0.58) × 10^2	337 (± 9.7)	0.439

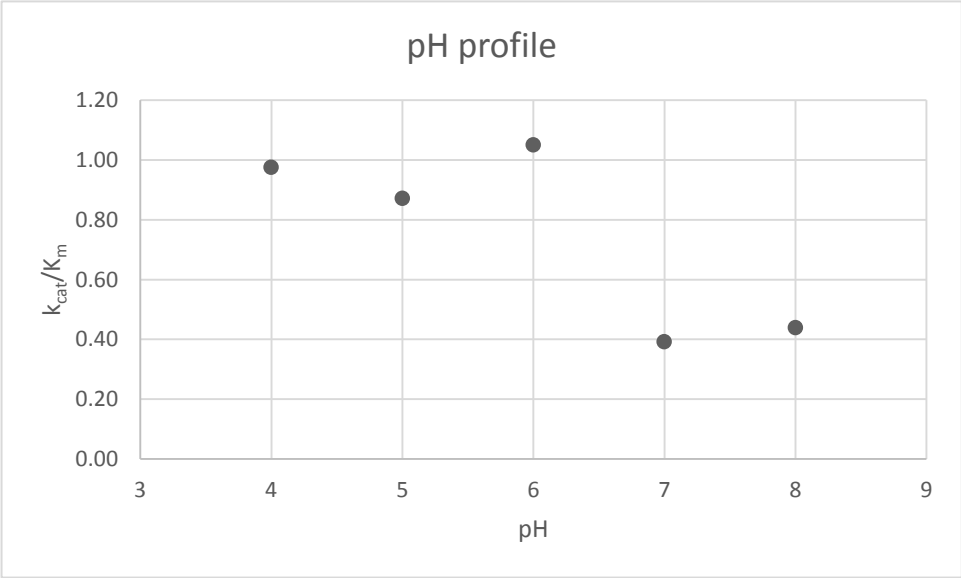

Figure 4.12. pH profile k_{cat}/K_m.

4.3 Investigation of ChiG activity on polysaccharides

A series of experiments were set up to investigate hydrolytic activity of ChiG towards a variety of polymeric soluble polysaccharides (see section 3.5.3). Activity was assayed by monitoring the elution profile of the polymeric substrate using size exclusion chromatography. Reasonable SEC chromatograms were obtained for arabinoxylan from wheat, cellulose, pectin, xylan from aspen, xanthan gum, betaglucan from barley, alginate, lichenan and galactomannan from guar, konjak and locus bean gum. The ChiG treatment did not affect the elution profile of any of these compounds (see an example in Figure 4.13).

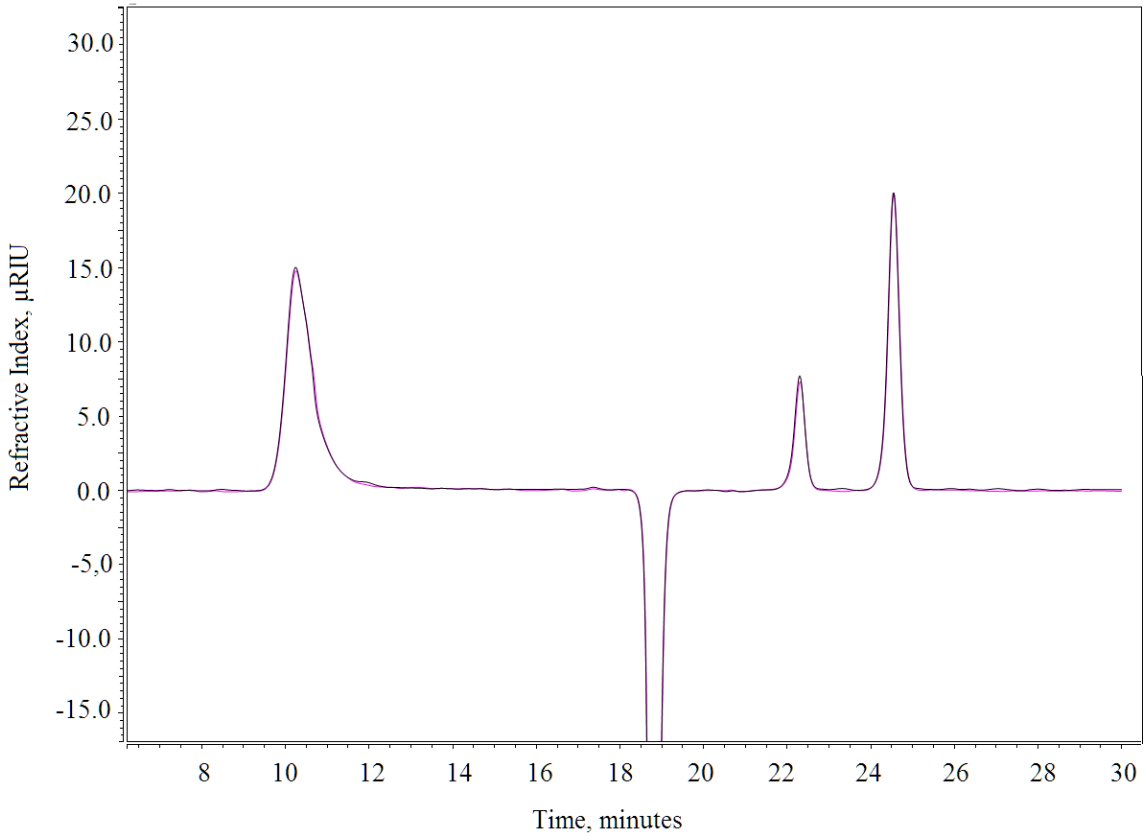

Figure 4.13 Example of chromatogram of elution profiles for a polysaccharide with and without ChiG treatment. The chromatogram for arabinoxylan from wheat is overlaid with the chromatogram for the same polysaccharide with ChiG treatment.

4.4 ChiG activity on bacterial cell wall polysaccharides

Activity of ChiG towards purified peptidoglycan from *S. pneumoniae* and cell wall fragments from *L. lactis*, *E. faecalis* and *L. plantarum* was analysed using MALDI-TOF MS analysis for detection of possible products. In addition to ChiG, both lysozyme and mutanolysin were assayed on the purified peptidoglycan and the cell wall fragments. A negative control containing no enzyme was also incorporated into the experiment. There were no noticeable difference between the mass spectra obtained from the peptidoglycan solutions treated with any of the enzymes and the negative controls, thus no soluble products were observed (see example in Figure 4.14).

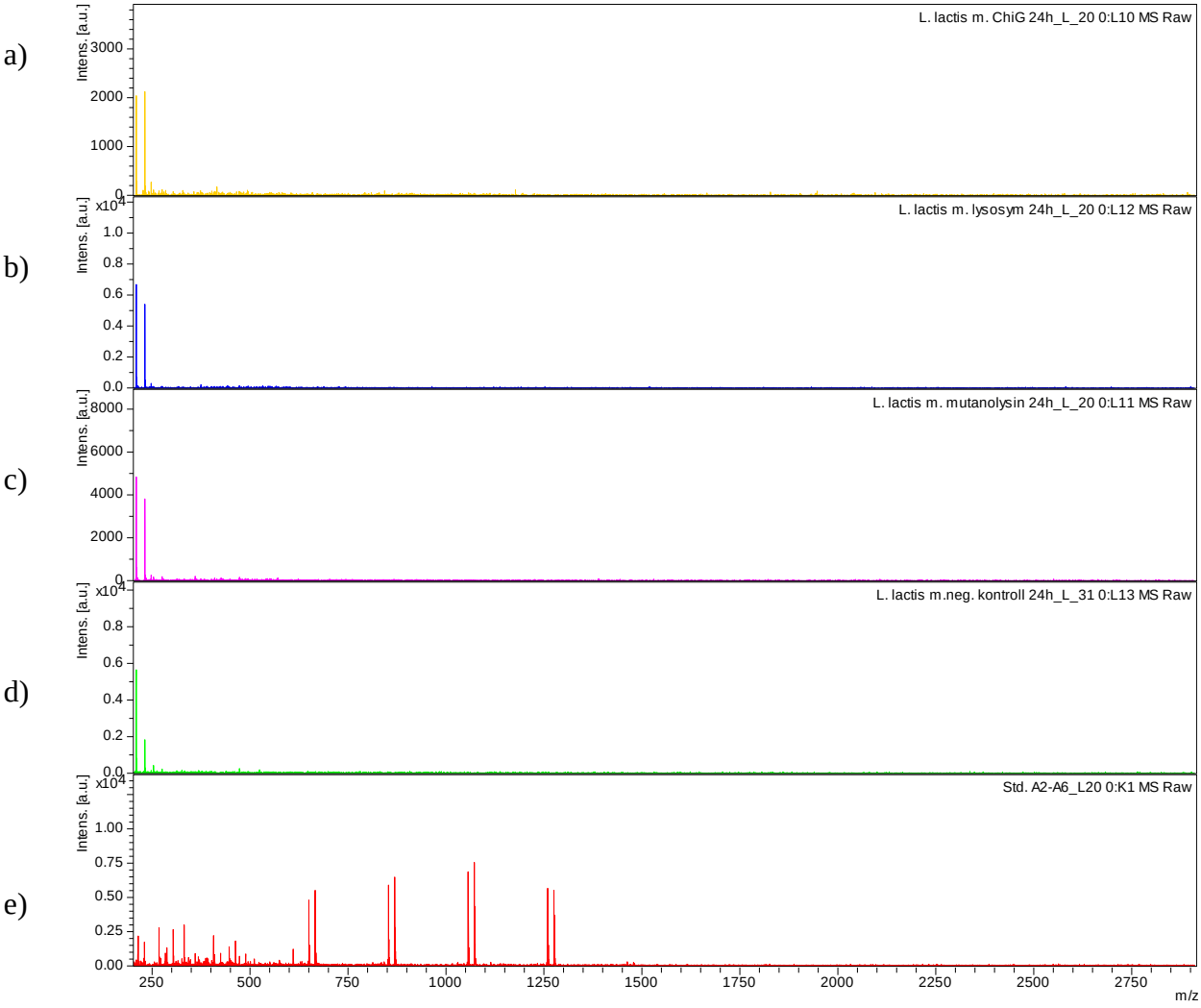

Figure 4.14. Example of mass spectra of soluble fractions obtained upon enzymatic degradation of bacterial cell wall fragments and peptidoglycan. The spectra are exemplified with potential degradation of cell wall fragments obtained from *L. lactis* after 24 hours incubation with the enzymes. a) ChiG activity. b) Lysozyme activity. c) Mutanolysin activity. d) Negative control, containing no enzyme. e) Standard containing di-, tri-, tetra-, penta- and hexachitooligosaccharides.

4.5 Antifungal activity of ChiG

Antifungal activity assays were performed using *T. reesei* QM6a as indicator organism, testing ChiG and a GH18 chitinase-rich preparation of the secretome of *S. marcescens*, to compare the two glycoside hydrolyse families of chitinases. Fungus was placed in the centre of the PDA plates when preparing the assays (according to section 3.9), with hyphae extending in all directions from this point. Four wells were punched in the agar around the fungus centre containing different enzyme concentrations, except one well that was used as a negative control only containing buffer. Figure 4.15 seems to shows no clear zone of inhibition of the hyphae (see the discussion section 5.3 for further details).

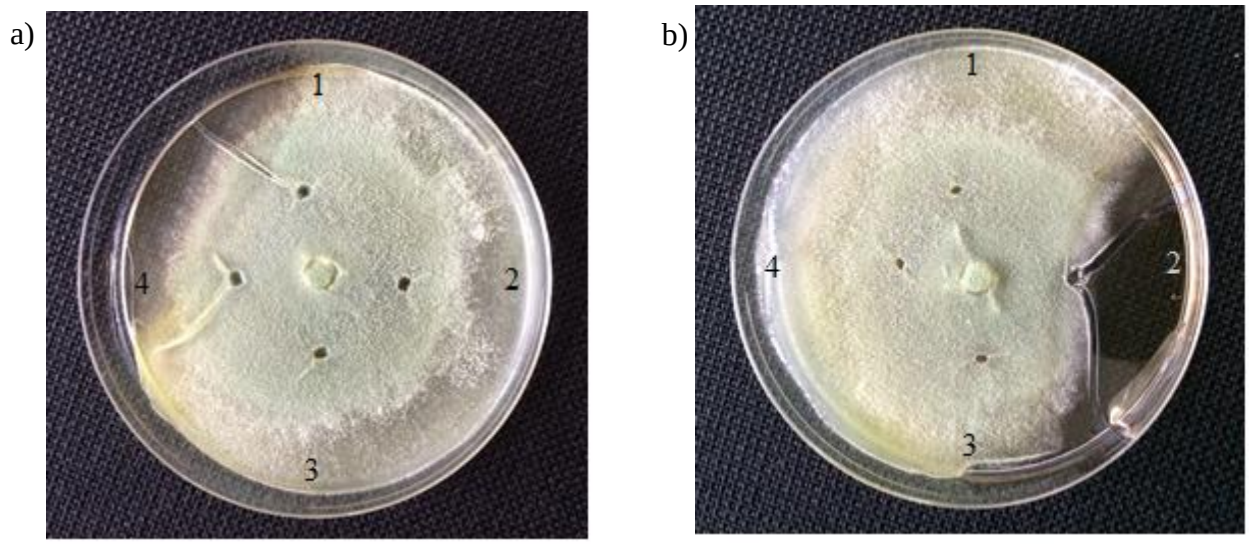

Figure 4.15. Antifungal assay. Fungi were applied to the plate by placing a fungus-containing agar plug in the middle of the plate, whereas chitinase solutions (30 µL, in 20 mM TrisHCl pH 8 buffer for ChiG and in 10 mM BisTris pH 6 buffer for the secretome of *S. marcescens*) were applied to the four punched holes, labeled 1 – 4. The pictures were taken after incubating the plates at 30 ºC for 40 hours total, but 18 hours after addition of the chitinase solutions. **Plate A**: Wells; 1, buffer only; 2, 7.16 µM ChiG; 3, 1.43 µM ChiG; 4, concentrated ChiG 35.82 µM. **Plate B**: Wells; 2, buffer only; 2, 0.55 mg/mL protein; 3, 0.11 mg/mL protein; 4, concentrated protein 2.75 mg/mL.

5 DISCUSSION

5.1 Overexpression and purification of ChiG

ChiG was successfully expressed and purified (Figures 4.1 and 4.3) from a periplasmic extract. However, when making the periplasmic extract, a considerable amount of the protein of interest was additionally observed in the pellet which contains cell rests including insoluble cytoplasmic proteins (Figure 4.2). This may be due to ChiG being produced at such a high level causing formation of insoluble particles of aggregated protein called inclusion bodies. Problems with inclusion bodies have previously been reported for ChiG (Heggset, 2005). Although ChiG could be purified from the periplasmic extract, it was decided to also attempt extraction of ChiG from cell lysates obtained by sonication. The pellet obtained after cell lysis by sonication also contained a great amount of ChiG, indicating the presence of inclusion bodies. However, the amount of soluble ChiG obtained was satisfactory and no further optimization of expression and protein extraction was conducted.

5.2 Substrate-binding in ChiG

Former activity measurements have shown that 4-methylumbelliferyl glycosides, often used as model substrates, cannot be used for family 19 glycoside hydrolases because of their mechanism of action (Gooday, 1999). Furthermore, kinetic parameters obtained with such artificial substrates may be affected by the non-natural chromophore (Krokeide et al., 2007). Hence, kinetic analysis was performed with chitooligosaccharides as substrates, which requires the use of advanced HPLC technologies for product identification and quantitation. K_m values for $(GlcNAc)_3$, $(GlcNAc)_4$ and $(GlcNAc)_5$ were high (see Table 4.1) compared to for example the GH18 chitinases chitinase A and B from *S. marcescens*, which have shown K_m values of 9 ± 1 µM and 4 ± 2 µM for $(GlcNAc)_4$ (Krokeide et al., 2007). The high K_m values indicates that ChiG does not bind very well to these substrates. Degradation of chitooligosaccharides with ChiG has previously been studied by measuring specific activity, which revealed that ChiG works better with longer substrates (Heggset, 2005).

The fact that the K_m values for the tetramer and the pentamer were similar indicates that the putative fifth (either -3 or +3) subsite is not important in binding the substrate. This finding is consistent with the conclusion that the bacterial GH19 chitinases only have four subsites (-2 to +2), which was derived from analysis of the ChiG crystal structure (Hoell et al., 2006). Hoell et al. did additionally confirme this conclusion with an anomeric analysis on degradation of $(GlcNAc)_5$ and $(GlcNAc)_6$, revealing similar α:β-ratios (~80:20) for the degradation products (2006).

Interestingly, the experimentally determined k_{cat} values (Table 4.1) are, like the K_m values, higher compared to reported kinetic parameters for the family 18 chitinases chitinase A (k_{cat} = 33 ± 1 s^{-1}) and chitinase B (k_{cat} = 28 ± 1 s^{-1}) from *S. marcescens* against $(GlcNAc)_4$ (Krokeide et al., 2007). The high k_{cat} values means that ChiG rapidly converts the substrate to product. k_{cat} values for $(GlcNAc)_4$ and $(GlcNAc)_5$ obtained in this thesis are in the same range, and degradation of $(GlcNAc)_6$ is previously reported to be in similar range of the tetramer and pentamer (Hoell et al., 2006) for ChiG . Despite the high k_{cat} values, the total efficiency of ChiG is lower compared to chitinase A (k_{cat}/K_m = 3.66) and chitinase B (k_{cat}/K_m = 7) in *S. marcescens* (Krokeide et al., 2007) because of the high K_m values.

One reason for the high k_{cat} values could be that GH19 enzymes distort the substrate, thus creating a higher conformational energy compared to the untwisted linkages, which may decrease the activation energy (Miyake et al., 2003). Recent studies on the GH19 chitinase from *B. coronatum* (moss) crystallized in complex with $(GlcNAc)_4$ showed a twist in the glycosidic linkage between the saccharides at the -1 and +1 subsites (Ohnuma et al., 2014). The chitinase in moss resembles the "loopless" structure of ChiG, and if the substrate in ChiG possesses the same twist upon binding, it could possibly contribute to the high degradation rate.

Kinetic analysis at different pH values showed that the kinetic parameters (k_{cat}/K_m) of ChiG change very little within the pH range tested. To inspect the pH profile of ChiG, pK_a values of the ionizable residues were obtained using the PROPKA software (Rostkowski et al., 2011). A list over the ionizable residues in or near the catalytic centre of ChiG, partially guided by a previous analysis of the ChiG-structure (Hoell, 2009) is shown in table 5.1. The estimated pK_a values of all investigated residues have values outside the range of tested pHs, except the catalytic acid and base. This is in accordance with the minimal effects the tested pH values have on the activity of ChiG. Hoell (2009) did also include an experiment calculating pK_a value of the catalytic acid in absence en presence of substrate. The experiment revealed that the pK_a value increased when the enzyme bound to the substrate.

Table 5.1. Ionizable residues in and near the catalytic center of ChiG. Residues were selected by inspection of the structure, partially guided by an analysis of Hoell et al. (2009). pK_a values were obtained using PROPKA software applied to the structure of ChiG (PDB: 2CJL) (Rostkowski et al., 2011)

Residue	**Function**	**pK_a**
Tyr86	Involved in -1 subsite	12.30
His67	Involved in +1 subsite	3.18
Glu68	Catalytic acid	5.40
Glu77	Catalytic base	4.49
Glu182	Important in catalysis	3.71
Arg194	Important in catalysis	10.52

The pH-activity profile (see Figure 4.12) for ChiG is atypical, in the sense that it is not showing the typical "bell-shape." This may be due to technical problems, or the use of different buffers affecting the catalytic rate. Despite the atypical shape, the pH profile seems to show a wide pH optimum, which is in accordance with a previous study that did attempt to make a pH activity profile for ChiG (Hoell, 2009). However, in the light of the results presented in this study, the pH activity profile reported by Hoell et al. was generated using too low substrate concentration (~0.5 mM), and even more important; chitosan (degree of acetylation 63 %) as a substrate. Chitosan has 37 % glucosamine, which contains a titratable amino group with a pK_a of approximately 6. Thus, the charge of the substrate will change with varying pH. In this thesis ChiG activity towards chitin tetrasaccharide is determined using kinetic parameters and is considered to provide more reliable results.

5.3 ChiG activity towards other substrates than chitin

The high K_m values towards the chitooligosaccharides are consistent to the hypothesis that ChiG may have another main substrate than chitin. Also, a previous study showed that a ChiG homologue (SACTE_0081) was expressed in the *Streptomyces sp.* SirexAA-E when grown on various carbon sources constituting plant cell walls (Takasuka et al., 2013), indicating that ChiG may have activity towards plant cell wall polysaccharides. Therefore, activity of ChiG towards a range of polysaccharides was tested for, but no activity was observed (Figure 4.13). However, no positive control was incorporated in the experiment which weakens the integrity of the results. ChiG has previously shown activity against chitosan, and this polysaccharide could therefore have been used as a positive control. Further, incubation of the substrates with ChiG happened in room temperature, which optimally should have been done at 37 ºC.

ChiG is structurally similar to lysozymes (Holm and Sander, 1994, Hart et al., 1993), which are known to degrade the peptidoglycan in cell walls. Therefore, purified peptidoglycan was tested, along with more crudely prepared cell wall fragments, using MALDI-TOF MS to analyse the potential degradation. A negative control without any enzyme was incorporated in the experiment, and lysozyme and mutanolysin was used as positive controls. Neither ChiG nor the positive controls showed any activity (Figure 4.14), and the experiment was therefore inconclusive. Positive controls not working may be due to the enzymes being inactive on the selected bacterial cell walls. Furthermore, during preparation of the cell wall fragments, it is possible that fragments were lost during the washing of the cells or that the cell wall fragments did not dissolve and remained in the pellet after the last centrifugation (which was discarded when preparing the substrate). For further work with ChiG on cell wall fragments, one must have functioning positive controls in order to verify the integrity of the assay.

Antifungal activity has previously been reported for the family 19 chitinases ChiC from *S. griseus* HUT (Itoh et al., 2002) and ChiF from *S. coelicolor* A3(2) (Kawase et al., 2006). ChiF and ChiG are the only two GH19 chitinases in *S. coelicolor* A3(2), and it was therefore interesting to determine whether ChiG also exhibited antifungal activity. As seen in Figure 4.18, hyphae from *T. reesei* have grown past the wells where ChiG was deposited, indicating that the enzyme does not inhibit hyphal growth. However, the result is difficult to interpret due to less growth observed between well 1 (containing no enzyme) and 4 (containing concentrated enzyme). An antifungal activity assay for the secretome of *S.marcescens*

containing family 18 chitinases was done for comparison, and is equally difficult to interpret due to less growth at well 2 (Figure 4.15). Clearly, the data in Fig. 4.18 are non-conclusive, e.g. because ruptures in the agar may be causing reduced growth in some areas. In a different procedure, enzyme solution were pipetted on paper disks placed on top of the agar, instead of punching wells into the medium (Watanabe et al., 1999). This method may reduce the risk of ruptures in the agar. Another improvement could be to check the plates earlier than 18 hour after depositing the enzyme to observe if hyphal inhibition does occur when hyphae has just passed the enzyme-containing wells.

A study comparing family 18 and 19 chitinases in *S. coelicolor* A3(2) showed that the selected bacterial family 18 chitinases did not exhibit antifungal activity (Kawase et al., 2006). However, chitinolytic enzymes from *S. marcescens* have previously shown antifungal activity (Someya et al., 2001), and it was therefore expected that the secretome of *S. marcescens* possible could inhibit hyphal extension. The selected family 19 chitinase (ChiF) in the comparative study (Kawase et al., 2006) did exhibit antifungal activity. Even though ChiG and ChiF are two family 19 chitinases found in the same organism, they differ by ChiF having a chitin-binding domain in addition to its catalytic domain, whereas ChiG does solely consist of a catalytic domain. ChiC from *S. Griseus* HUT6037 is structurally similar to the multidomain ChiF and has shown antifungal activity as well (Itoh et al., 2002). However, upon deleting the chitin-binding domain ChiC did not show antifungal activity (Itoh et al., 2002). The hypothesis of the chitin-binding domain being important in antifungal activity is strengthened by the antifungal assay of ChiG which seems to show that ChiG does not inhibit hyphal extension. However, the antifungal assay should be improved by following the above-mentioned suggestions before making a final conclusion as to the antifungal activity of ChiG. It should be noted that only one fungus was tested in this study. Fungi are diverse in terms of composition and the amount of chitin in cell wall, thus further research could include testing ChiG against various fungi.

5.4 Concluding remarks and future perspectives

This thesis describes a kinetic and functional characterization of the bacterial family 19 chitinase, ChiG. The high K_m of ChiG may indicate a preference for a substrate different than chitin, but the high k_{cat} also signals that the β−1,4 glycosidic bond between two *N*-acetylglucosamines (as in the case for chitin) being the main target. Although a great amount of potential substrate targets were tested against ChiG, more research is indeed needed to understand the biological roles of these enzymes. Such research could include studying transcription/secretion of ChiG in *S. coelicolor* A3(2) when grown on various substrates such as plant cell walls, chitin or non-living bacteria. If ChiG then is found to be upregulated/secreted, it may be easier to identify the substrate it is acting on.

Importantly, the kinetic data obtained in this study are quite unique, giving new insight into family 19 chitinases. In light of the present study, the mutational study by Hoell et al. (2009) was done using too low substrate concentrations when testing mutants and wild-type ChiG against $(GlcNAc)_6$. Effects caused by K_m or k_{cat} cannot be distinguished, thus new analyses are required.

All in all, the function of ChiG, and family 19 chitinases in general remains somewhat unclear.

6 REFERENCES

BENTLEY, S., CHATER, K., CERDENO-TARRAGA, A.-M., CHALLIS, G., THOMSON, N., JAMES, K., HARRIS, D., QUAIL, M., KIESER, H. & HARPER, D. 2002. Complete genome sequence of the model actinomycete Streptomyces coelicolor A3 (2). *Nature,* 417**,** 141-147.

BRADFORD, M. M. 1976. A rapid and sensitive method for the quantitation of microgram quantities of protein utilizing the principle of protein-dye binding. *Analytical biochemistry,* 72**,** 248-254.

BRAMELD, K. A. & GODDARD, W. A. 1998. The role of enzyme distortion in the single displacement mechanism of family 19 chitinases. *Proceedings of the National Academy of Sciences,* 95**,** 4276-4281.

BROGUE, K., CHET, I., HOLLIDAY, M., CRESSMAN, R., BIDDLE, P., KNOWLTON, S., MAUVAIS, C. J. & BROGLIE, R. 1991. Transgenic plants with enhanced resistance to the fungal pathogen Rhizoctonia solani. *Science,* 254**,** 1194-1197.

BUEREN, A. L. V. 2013. *Carbohydrate-binding modules* [Online]. CAZypedia. Available: http://www.cazypedia.org/index.php/Carbohydrate-binding_modules [Accessed 4/24 2014].

COLLINGE, D. B., KRAGH, K. M., MIKKELSEN, J. D., NIELSEN, K. K., RASMUSSEN, U. & VAD, K. 1993. Plant chitinases. *The Plant Journal,* 3**,** 31-40.

DAMODARAN, S., PARKIN, K. & FENNEMA, O. R. 2008. *Fennema's food chemistry,* Boca Raton, Taylor & Francis.

DAVIES, G. & HENRISSAT, B. 1995. Structures and mechanisms of glycosyl hydrolases. *Structure,* 3**,** 853-859.

DAVIES, G. J., GLOSTER, T. M. & HENRISSAT, B. 2005. Recent structural insights into the expanding world of carbohydrate-active enzymes. *Current opinion in structural biology,* 15**,** 637-645.

DELANO, W. L. 2002. The PyMOL molecular graphics system.

ENGEL, P. C. 1977. *Enzyme kinetics: the steady-state approach,* London, Chapman & Hall.

GARDNER, K. & BLACKWELL, J. 1975. Refinement of the structure of β-chitin. *Biopolymers,* 14**,** 1581-1595.

GOODAY, G. W. 1990. The ecology of chitin degradation. *Advances in microbial ecology.* Springer.

GOODAY, G. W. 1999. Aggressive and defensive roles for chitinases. *Chitin and Chitinases.* Springer.

HAHN, M., HENNIG, M., SCHLESIER, B. & HOHNE, W. 2000. Structure of jack bean chitinase. *Acta Crystallographica Section D: Biological Crystallography,* 56**,** 1096-1099.

HART, P. J., MONZINGO, A. F., READY, M. P., ERNST, S. R. & ROBERTUS, J. D. 1993. Crystal Structure of an Endochitinase from< i> Hordeum vulgare</i> L. Seeds. *Journal of molecular biology,* 229**,** 189-193.

HEGGSET, E. B. 2005. *Overuttrykk av familie 19 kitinaser fra gran (Picea abies) og Streptomyces coelicolor A3(2): og detaljert karakterisering av Streptomyces enzymet ChiG,* Ås, [E.B. Heggset].

HENRISSAT, B. & DAVIES, G. 1997. Structural and sequence-based classification of glycoside hydrolases. *Current opinion in structural biology,* 7**,** 637-644.

HOELL, I. A. 2009. *Characterization of enzymes that act on chitin and related polymers,* Ås, Universitetet for miljø- og biovitenskap, UMB.

HOELL, I. A., DALHUS, B., HEGGSET, E. B., ASPMO, S. I. & EIJSINK, V. G. 2006. Crystal structure and enzymatic properties of a bacterial family 19 chitinase reveal differences from plant enzymes. *FEBS Journal,* 273**,** 4889-4900.

HOELL, I. A., VAAJE-KOLSTAD, G. & EIJSINK, V. G. 2010. Structure and function of enzymes acting on chitin and chitosan. *Biotechnology and Genetic Engineering Reviews,* 27**,** 331-366.

HOLM, L. & SANDER, C. 1994. Structural similarity of plant chitinase and lysozymes from animals and phage: an evolutionary connection. *FEBS letters,* 340**,** 129-132.

HONG, J. K. & HWANG, B. K. 2002. Induction by pathogen, salt and drought of a basic class II chitinase mRNA and its in situ localization in pepper (Capsicum annuum). *Physiologia plantarum,* 114**,** 549-558.

HUET, J., RUCKTOOA, P., CLANTIN, B., AZARKAN, M., LOOZE, Y., VILLERET, V. & WINTJENS, R. 2008. X-ray Structure of Papaya Chitinase Reveals the Substrate Binding Mode of Glycosyl Hydrolase Family 19 Chitinases†‡. *Biochemistry,* 47**,** 8283-8291.

ITOH, Y., KAWASE, T., NIKAIDOU, N., FUKADA, H., MITSUTOMI, M. & WATANABE, T. 2002. Functional analysis of the chitin-binding domain of a family 19 chitinase from Streptomyces griseus HUT6037: substrate-binding affinity and cis-dominant increase of antifungal function. *Bioscience, biotechnology, and biochemistry,* 66**,** 1084-1092.

IUBMB. 2013. *Recommendations on Biochemical & Organic Nomenclature, Symbols & Terminology etc.* [Online]. London: School of Biological and Chemical Sciences, Mart Queen University of London. Available: http://www.chem.qmul.ac.uk/iubmb/ [Accessed 2/9 2013].

JOHN HART, P., PFLUGER, H. D., MONZINGO, A. F., HOLLIS, T. & ROBERTUS, J. D. 1995. The refined crystal structure of an endochitinasefrom< i> Hordeum vulgare</i> L. seeds at 1.8 Å resolution. *Journal of molecular biology,* 248**,** 402-413.

KAWASE, T., SAITO, A., SATO, T., KANAI, R., FUJII, T., NIKAIDOU, N., MIYASHITA, K. & WATANABE, T. 2004. Distribution and phylogenetic analysis of family 19 chitinases in Actinobacteria. *Applied and environmental microbiology,* 70**,** 1135-1144.

KAWASE, T., YOKOKAWA, S., SAITO, A., FUJII, T., NIKAIDOU, N., MIYASHITA, K. & WATANABE, T. 2006. Comparison of enzymatic and antifungal properties between family 18 and 19 chitinases from S. coelicolor A3 (2). *Bioscience, biotechnology, and biochemistry,* 70**,** 988-998.

KEZUKA, Y., OHISHI, M., ITOH, Y., WATANABE, J., MITSUTOMI, M., WATANABE, T. & NONAKA, T. 2006. Structural Studies of a Two-domain Chitinase from< i> Streptomyces griseus</i> HUT6037. *Journal of molecular biology,* 358**,** 472-484.

KOSHLAND, D. E. 1953. Stereochemistry and the mechanism of enzymatic reactions. *Biological Reviews,* 28**,** 416-436.

KROKEIDE, I.-M., SYNSTAD, B., GÅSEIDNES, S., HORN, S. J., EIJSINK, V. G. & SØRLIE, M. 2007. Natural substrate assay for chitinases using high-performance liquid chromatography: a comparison with existing assays. *Analytical biochemistry,* 363**,** 128-134.

LAEMMLI, U. 1970. Cleavage of structural proteins during the assembly of the head of bacteriophage T4 Nature 227: 680–685.

MERZENDORFER, H. & ZIMOCH, L. 2003. Chitin metabolism in insects: structure, function and regulation of chitin synthases and chitinases. *Journal of Experimental Biology,* 206**,** 4393-4412.

MILLER, J. M. 2005. *Chromatography: concepts and contrasts,* Hoboken, N.J., Wiley.
MINKE, R. & BLACKWELL, J. 1978. The structure of α-chitin. *Journal of molecular biology,* 120**,** 167-181.
MIYAKE, H., KURISU, G., KUSUNOKI, M., NISHIMURA, S., KITAMURA, S. & NITTA, Y. 2003. Crystal structure of a catalytic site mutant of β-amylase from Bacillus cereus var. mycoides cocrystallized with maltopentaose. *Biochemistry,* 42**,** 5574-5581.
MONZINGO, A. F., MARCOTTE, E. M., HART, P. J. & ROBERTUS, J. D. 1996. Chitinases, chitosanases, and lysozymes can be divided into procaryotic and eucaryotic families sharing a conserved core. *Nature structural biology,* 3**,** 133-140.
MUZZARELLI, R. A. 2011. Chitin nanostructures in living organisms. *Chitin.* Springer.
OHNO, T., ARMAND, S., HATA, T., NIKAIDOU, N., HENRISSAT, B., MITSUTOMI, M. & WATANABE, T. 1996. A modular family 19 chitinase found in the prokaryotic organism Streptomyces griseus HUT 6037. *Journal of bacteriology,* 178**,** 5065-5070.
OHNUMA, T., UMEMOTO, N., KONDO, K., NUMATA, T. & FUKAMIZO, T. 2013. Complete subsite mapping of a "loopful" GH19 chitinase from rye seeds based on its crystal structure. *FEBS letters,* 587**,** 2691-2697.
OHNUMA, T., UMEMOTO, N., NAGATA, T., SHINYA, S., NUMATA, T., TAIRA, T. & FUKAMIZO, T. 2014. Crystal structure of a "loopless" GH19 chitinase in complex with chitin tetrasaccharide spanning the catalytic center. *Biochimica et Biophysica Acta (BBA)-Proteins and Proteomics,* 1844**,** 793-802.
PIHAKASKI-MAUNSBACH, K., MOFFATT, B., TESTILLANO, P., RISUEÑO, M., YEH, S., GRIFFITH, M. & MAUNSBACH, A. B. 2001. Genes encoding chitinase-antifreeze proteins are regulated by cold and expressed by all cell types in winter rye shoots. *Physiologia plantarum,* 112**,** 359-371.
PRAKASH, N. U., JAYANTHI, M., SABARINATHAN, R., KANGUEANE, P., MATHEW, L. & SEKAR, K. 2010. Evolution, homology conservation, and identification of unique sequence signatures in GH19 family chitinases. *Journal of molecular evolution,* 70**,** 466-478.
RINAUDO, M. 2006. Chitin and chitosan: properties and applications. *Progress in polymer science,* 31**,** 603-632.
ROSTKOWSKI, M., OLSSON, M. H., SØNDERGAARD, C. R. & JENSEN, J. H. 2011. Graphical analysis of pH-dependent properties of proteins predicted using PROPKA. *BMC structural biology,* 11**,** 6.
RÄSÄNEN, L. & ARVILOMMI, H. 1981. Cell walls, peptidoglycans, and teichoic acids of gram-positive bacteria as polyclonal inducers and immunomodulators of proliferative and lymphokine responses of human B and T lymphocytes. *Infection and immunity,* 34**,** 712-717.
SAITO, A., FUJII, T., YONEYAMA, T., REDENBACH, M., OHNO, T., WATANABE, T. & MIYASHITA, K. 1999. High-multiplicity of chitinase genes in Streptomyces coelicolor A3 (2). *Bioscience, biotechnology, and biochemistry,* 63**,** 710-718.
SAITO, A., ISHIZAKA, M., FRANCISCO, P. B., FUJII, T. & MIYASHITA, K. 2000. Transcriptional co-regulation of five chitinase genes scattered on the Streptomyces coelicolor A3 (2) chromosome. *Microbiology,* 146**,** 2937-2946.
SEGEL, I. H. 1993. *Enzyme kinetics: behavior and analysis of rapid equilibrium and steady-state enzyme systems,* New York, Wiley.
SINNOTT, M. L. 1990. Catalytic mechanism of enzymic glycosyl transfer. *Chemical Reviews,* 90**,** 1171-1202.

SOMEYA, N., NAKAJIMA, M., HIRAYAE, K., TADAAKI, H. & AKUTSU, K. 2001. Synergistic antifungal activity of chitinolytic enzymes and prodigiosin produced by biocontrol bacterium, Serratia marcescens strain B2 against gray mold pathogen, Botrytis cinerea. *Journal of general plant pathology,* 67**,** 312-317.

TAIRA, T., MAHOE, Y., KAWAMOTO, N., ONAGA, S., IWASAKI, H., OHNUMA, T. & FUKAMIZO, T. 2011. Cloning and characterization of a small family 19 chitinase from moss (Bryum coronatum). *Glycobiology,* 21**,** 644-654.

TAKASUKA, T. E., BOOK, A. J., LEWIN, G. R., CURRIE, C. R. & FOX, B. G. 2013. Aerobic deconstruction of cellulosic biomass by an insect-associated Streptomyces. *Scientific reports,* 3.

UBHAYASEKERA, W., RAWAT, R., HO, S. W. T., WIWEGER, M., VON ARNOLD, S., CHYE, M.-L. & MOWBRAY, S. L. 2009. The first crystal structures of a family 19 class IV chitinase: the enzyme from Norway spruce. *Plant molecular biology,* 71**,** 277-289.

VAAJE-KOLSTAD, G., WESTERENG, B., HORN, S. J., LIU, Z., ZHAI, H., SØRLIE, M. & EIJSINK, V. G. 2010. An oxidative enzyme boosting the enzymatic conversion of recalcitrant polysaccharides. *Science,* 330**,** 219-222.

VENTURA, M., CANCHAYA, C., TAUCH, A., CHANDRA, G., FITZGERALD, G. F., CHATER, K. F. & VAN SINDEREN, D. 2007. Genomics of Actinobacteria: tracing the evolutionary history of an ancient phylum. *Microbiology and Molecular Biology Reviews,* 71**,** 495-548.

WATANABE, T., KANAI, R., KAWASE, T., TANABE, T., MITSUTOMI, M., SAKUDA, S. & MIYASHITA, K. 1999. Family 19 chitinases of Streptomyces species: characterization and distribution. *Microbiology,* 145**,** 3353-3363.

ZHONG, R., KAYS, S. J., SCHROEDER, B. P. & YE, Z.-H. 2002. Mutation of a chitinase-like gene causes ectopic deposition of lignin, aberrant cell shapes, and overproduction of ethylene. *The Plant Cell Online,* 14**,** 165-179.

APPENDIX

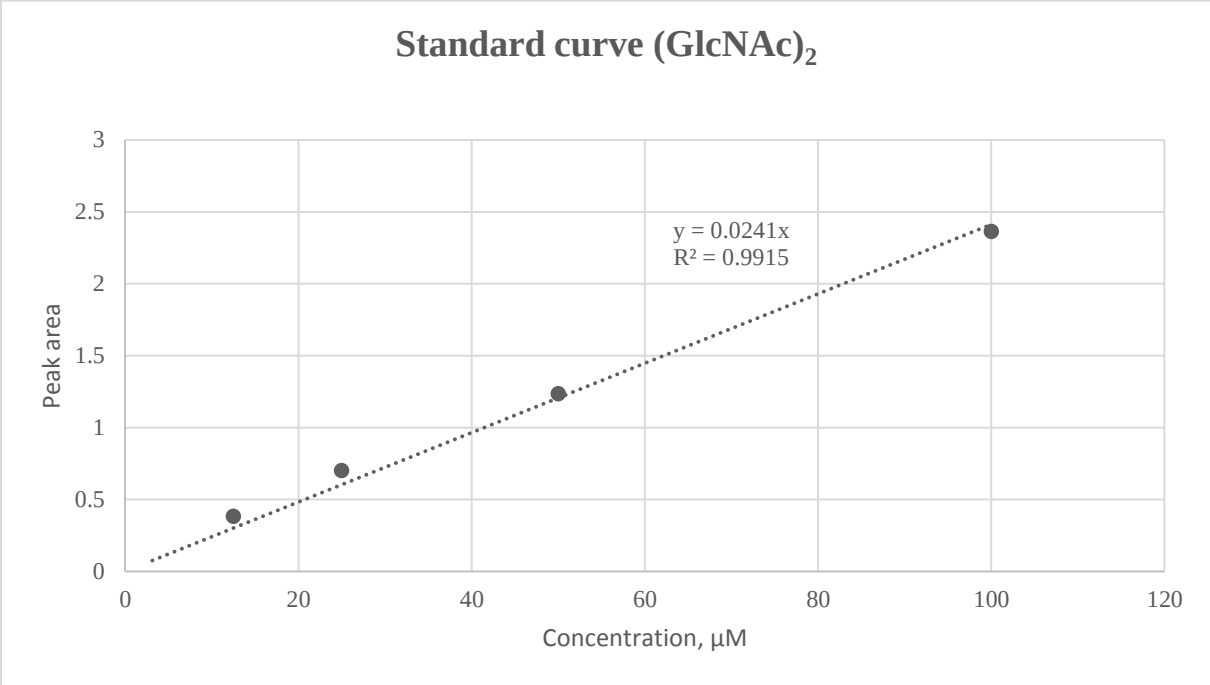

Figure A1. Standard curve for $(GlcNAc)_2$.

Table A1. R-values for the experimentally determined velocities at each substrate concentration used in the Michaelis-Menten plots. The velocity was calculated by plotting measured absorbance versus minutes, and a linear correlation was expected. The R-value describes this linearity, which optimally should be close to 1.

Experiment	Concentration, µM	Parallel 1	Parallel 2	Parallel 3
$(GlcNAc)_3$ assay pH 6	300	0,99	0,99	-
	600	0,99	0,99	-
	900	0,99	0,99	-
	1800	0,99	1,00	-
	3600	0,99	1,00	-
	5400	0,99	1,00	-
$(GlcNAc)_4$ assay pH 6	100	0,99	0,89	0,96
	200	0,98	0,94	0,98
	400	0,98	0,98	0,96
	600	0,99	0,98	0,99
	1000	0,99	0,98	0,98
	1400	0,98	0,98	0,97
	2000	0,98	0,94	0,95
	3000	0,98	0,93	0,97
$(GlcNAc)_5$ assay pH 6	100	0,98	0,99	0,98
	200	1,00	0,99	0,99
	400	0,96	0,96	0,96
	600	0,97	0,95	0,93
	800	0,86	0,95	0,90
	1200	0,92	0,94	0,82
	2000	0,84	0,86	0,86
$(GlcNAc)_4$ assay pH 4	100	0,98	0,98	0,98
	200	0,98	0,98	0,99
	400	0,99	0,99	0,99
	600	0,99	0,99	0,99
	1000	0,99	0,99	0,98
	1400	0,99	1,00	0,99
	2000	1,00	0,99	0,99
	3000	0,99	0,99	0,97
$(GlcNAc)_4$ assay pH 5	100	0,97	0,97	0,98
	200	0,98	0,98	0,98
	400	0,97	0,98	0,98
	600	0,98	0,98	0,98
	1000	0,95	0,97	0,97
	1400	0,95	0,96	0,96
	2000	0,96	0,96	0,97
	3000	0,93	0,95	0,94

$(GlcNAc)_4$ assay pH 7	100	0,97	0,98	0,97
	200	0,95	0,96	0,97
	400	0,97	0,98	0,95
	600	0,97	0,97	0,96
	1000	0,98	0,96	0,96
	1400	0,96	0,96	0,94
	2000	0,94	0,90	0,96
	3000	0,88	0,90	0,92
$(GlcNAc)_4$ assay pH 8	100	0,99	0,99	0,98
	200	1,00	1,00	1,00
	400	0,99	0,99	0,99
	600	0,99	0,99	0,98
	1000	0,99	0,98	0,97
	1400	0,98	0,97	0,96
	2000	0,97	0,93	0,96
	3000	0,95	0,95	0,87

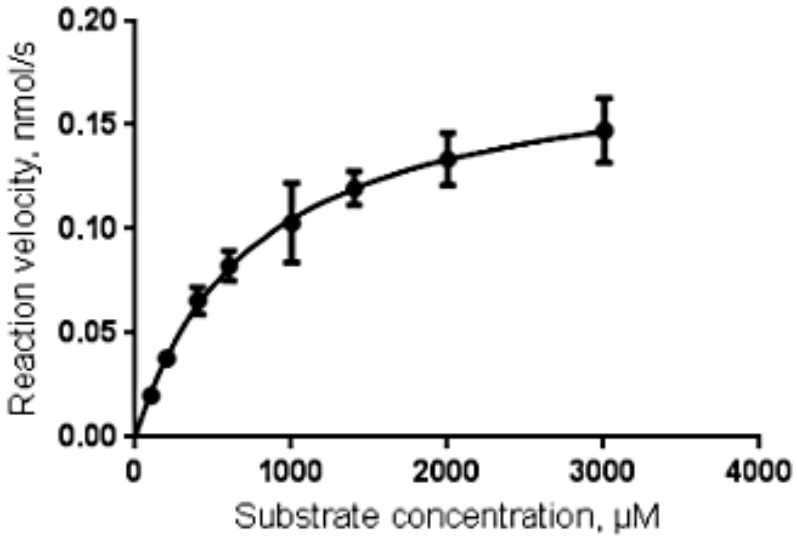

Figure A2. Michaelis-Menten plot of ChiG activity towards $(GlcNAc)_4$ at pH 4.

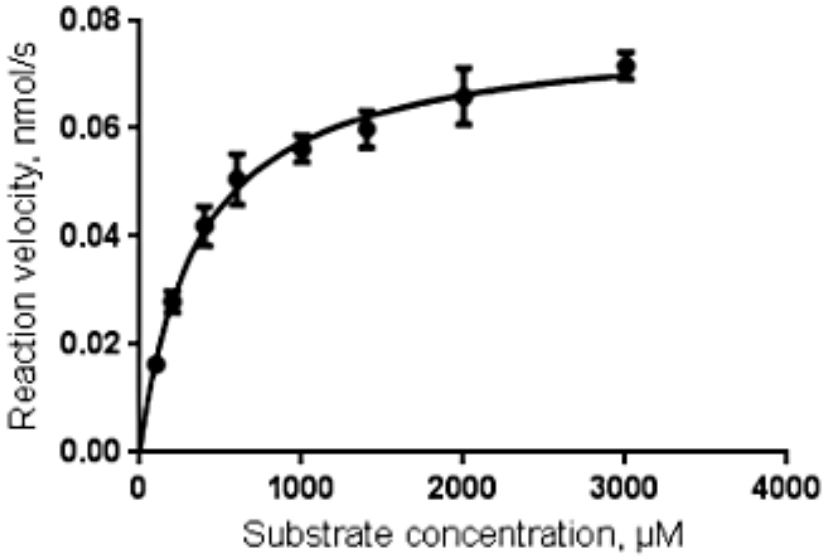

Figure A3. Michaelis-Menten plot of ChiG activity towards $(GlcNAc)_4$ at pH 5.

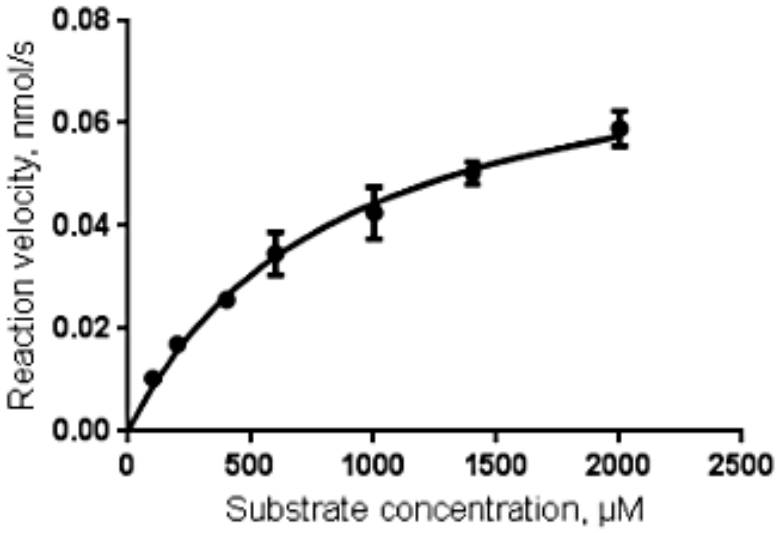

Figure A4. Michaelis-Menten plot of ChiG activity towards $(GlcNAc)_4$ at pH 7.

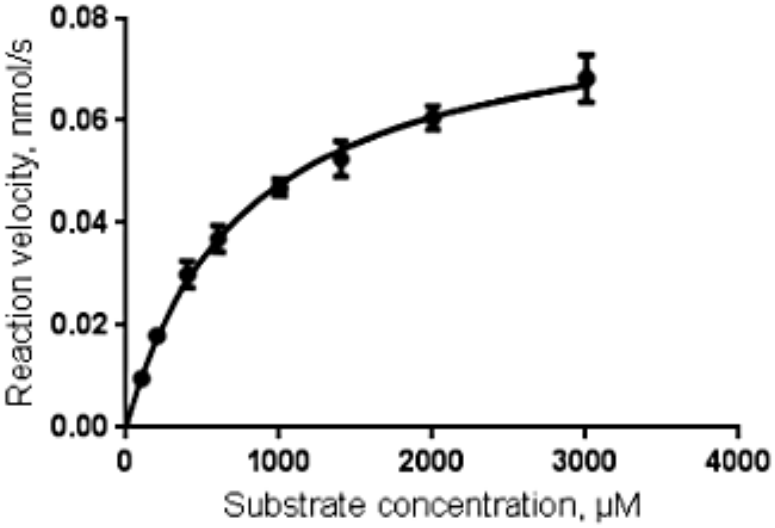

Figure A5. Michaelis-Menten plot of ChiG activity towards $(GlcNAc)_4$ at pH 8

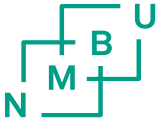

Norwegian University
of Life Sciences

Postboks 5003
NO-1432 Ås, Norway
+47 67 23 00 00
www.nmbu.no